



OPEN

Novel psoralen derivatives as anti-breast cancer agents and their light-activated cytotoxicity against HER2 positive breast cancer cells

Chiphada Aekrungrueangkit¹, Sirilak Wangngae², Anyanee Kamkaew², Ruchuta Ardkhean³, Sanit Thongnest^{4,5}, Jutatip Boonsombat^{4,5}✉, Somsak Ruchirawat^{4,5,6} & Tanatorn Khotavivattana¹✉

Psoralen derivatives are well known for their unique phototoxicity and also exhibits promising anti-breast cancer activity both in the presence and the absence of UVA irradiation. However, the structure–activity relationship on this scaffold remains lacking. Herein, a series of psoralen derivatives with various C-5 substituents were synthesized and evaluated for their in vitro dark and light-activated cytotoxicity against three breast cancer cell lines: MDA-MB-231, T47-D, and SK-BR-3. The type of substituents dramatically impacted the activity, with the 4-bromobenzyl amide derivative (3c) exhibiting the highest dark cytotoxicity against T47-D ($IC_{50} = 10.14 \mu\text{M}$), with the activity comparable to those of the reference drugs (doxorubicin, $1.46 \mu\text{M}$; tamoxifen citrate, $20.86 \mu\text{M}$; lapatinib $9.78 \mu\text{M}$). On the other hand, the furanylamide 3g exhibits the highest phototoxicity against SK-BR-3 cells with the IC_{50} of $2.71 \mu\text{M}$, which is almost tenfold increase compared to the parent compound, methoxsalen. Moreover, these derivatives showed exceptional selectivity towards HER2+ (SK-BR-3) over the HER2– (MDA-MB-231) breast cancer cell lines, which correlates well with the results from the molecular docking study, revealing that 3g formed favorable interactions within the active site of the HER2. Additionally, the cell morphology of SK-BR-3 cells suggested that the significant phototoxicity was related to induction of cell apoptosis. Most of the synthesized psoralen derivatives possess acceptable physicochemical properties and are suitable for being further developed as a novel anti-breast cancer agent in the future.

Breast cancer is currently a major global health concern with high incidence and mortality rate in women, as there were 2.26 million cases reported in 2020, with the ASR (Age Standardized Incidence Rate per 100,000 people) as high as 47.8, according to the World Health Organization (WHO)¹. Both chemotherapy and phototherapy have been regularly used for the treatment of breast cancer, especially in the breast-conserving therapy (BCT), and also in combination with surgery². However, the effectiveness drops dramatically if the tumors are detected in the later stages. Moreover, these methods also suffer from a certain degree of limitations such as toxic side effects stemming from the limited selectivity of the currently available anti-cancer drugs^{3,4}, as well as the lack of efficacy due to the development of resistance in some breast cancer strains⁵. Consequently, the development of novel anti-breast cancer agents with high efficacy, selectivity, and biocompatibility is highly in demand.

For the past few decades, furocoumarin, a class of heterocyclic compound containing a furan fused with a coumarin, has proved to be a promising chemical scaffold for the development of novel drugs against breast

¹Center of Excellence in Natural Products Chemistry, Department of Chemistry, Faculty of Science, Chulalongkorn University, Bangkok 10330, Thailand. ²School of Chemistry, Institute of Science, Suranaree University of Technology, Nakhon Ratchasima 30000, Thailand. ³Princess Srisavangavadhana College of Medicine, Chulabhorn Royal Academy, Bangkok 10210, Thailand. ⁴Chulabhorn Research Institute, Bangkok 10210, Thailand. ⁵Center of Excellence on Environmental Health and Toxicology (EHT), OPS, MHESI, Bangkok, Thailand. ⁶Program in Chemical Sciences, Chulabhorn Graduate Institute, Chulabhorn Royal Academy, Bangkok 10210, Thailand. ✉email: jutatip@cri.or.th; tanatorn.k@chula.ac.th

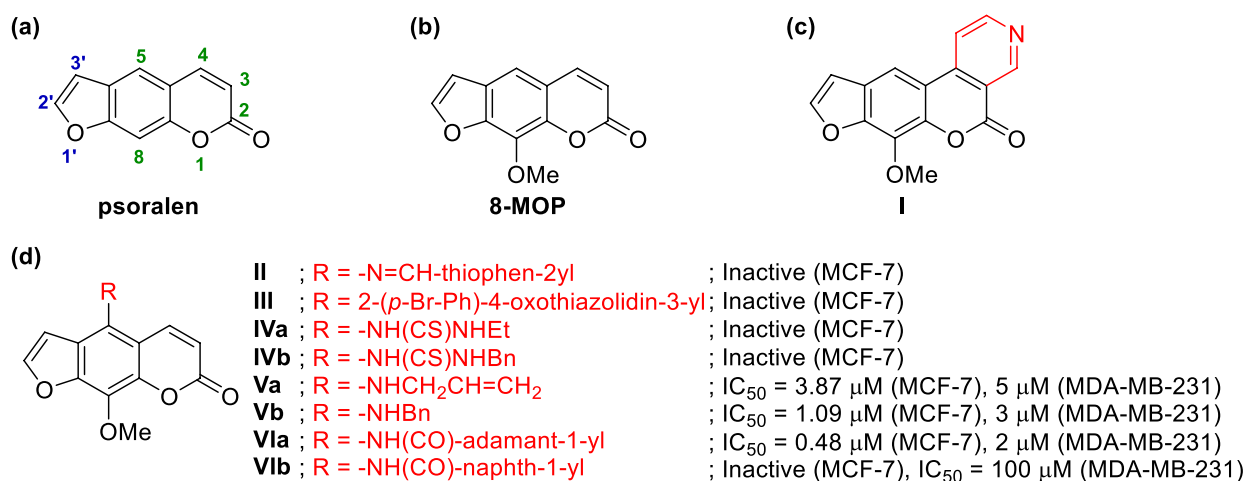


Figure 1. Example of psoralen derivatives and their anti-cancer activity.

cancer⁶. In early dates, natural-occurring psoralen (linear furocoumarin; Fig. 1a) derivatives such as 8-methoxypsoralen (8-MOP; Fig. 1b) were utilized clinically in a photochemotherapy⁷, due to their ability to intercalate DNA causing interstrand DNA crosslinks (ICL) upon photo-activated by UV irradiation, and hence inhibiting transcription and DNA replication⁸. This concept known as PUVA (psoralen and ultraviolet A) therapy is extensively used for the treatment of epidermal proliferative and inflammatory disorders⁹, and was shown to exert anti-proliferative effects in some breast cancer cell lines¹⁰. However, recent studies on psoralen derivative I incapable of inducing ICL formation (Fig. 1c) revealed the evidence that the anti-cancer effects of PUVA can also be mediated through a DNA-independent mechanism, involving the direct binding of psoralen with the catalytic autokinase domain of human epidermal growth factor receptor 2 (HER2; also known as erythroblastic oncogene B or ErbB2)¹¹. This mechanism of action reflects in the high selectivity of PUVA towards HER2-overexpressing breast cancer cells such as SK-BR-3, which are known to be more aggressive and have a greater risk for disease progression¹². However, the structure–activity relationship (SAR) study on the PUVA against breast carcinoma has never been reported.

Apart from photoactivation, psoralen derivatives have been demonstrated to possess moderate activity against breast cancer cell lines even in the absence of radiation¹³. Previous studies on the synthesis of novel psoralen derivatives focused on the structural modification at the C-5 position with substituents ranging from immine (II)¹⁴, thiazolidine (III)¹⁴, thiourea (IV)¹⁴, amine (V)¹⁵, and amide (VI)¹⁵, as shown in Fig. 1d. Among them, the amide derivative VIa bearing adamantoyl group exhibited promising activity towards both estrogenic (MCF-7) and non-estrogenic (MDA-MB-231) breast cancer cell lines, while little to no activity was found in the naphthoyl derivative VIb. The stark contrast in the activity, together with the lack of the scope of substituents encouraged us to further explore this amide series. Herein, we report the synthesis and anti-breast cancer activity of novel psoralen derivatives bearing different types of amide and other substituents against both hormone-dependent (T47-D) and hormone-independent (MDA-MB-231) breast cancer cells, compared with the normal cells. Moreover, since these derivatives have never been tested under UV irradiation, we also explored their phototoxicity against both HER2+ (SK-BR-3) and HER2– (MDA-MB-231) breast cancer cell lines. Since the actual targets are not unequivocally proven, we also carried out molecular docking with a potential protein target; HER2, in order to shed light on the potential binding interactions of these psoralen derivatives. Finally, the physicochemical properties, the essential parameters for discovering and developing new drugs, of these novel psoralen derivatives were also investigated.

Results and discussion

Synthesis of psoralen derivatives. Four types of psoralen derivatives including amides (3a–n), amines (4a–b), sulfonamide (5), and thiourea (6) were synthesized following the synthetic route shown in Fig. 2. First, the commercially available 8-MOP was converted into the 5-nitro analog 1, which was then reduced into the 5-amino analog 2 using tin powder as a reducing agent^{16,17}. Next, 2 was treated with different acid chlorides or acid anhydrides to afford the corresponding amide derivatives 3a–n with the yields ranging from 15 to 98%. Since the previous work reported that the amide derivatives showed promising results against breast cancer cell lines¹⁵, in this work we then emphasized on the structure variation of the amide derivatives, with the substitution patterns ranging from aromatic amides bearing substituents with various electronic and steric effects (3a–f), heteroaromatic amides (3g–h), and aliphatic amides with different carbon chain lengths (3i–n). The adamantoyl derivative 3n (VIa), the best compound reported in the literature¹⁵, was also included as a control. Notably, the acylation using hexanoyl chloride resulted in the unusual disubstituted analog 3m in 21% yield as confirmed by spectroscopic analysis. Apart from the amide derivatives, the amine analogs 4a and 4b bearing benzyl and 4-bromobenzyl substituents, respectively, were synthesized by the alkylation of 2 in moderate yields¹⁵. The sulfonation of 2 with benzenesulfonyl chloride afforded sulfonamide derivative 5 in 82% yield¹⁸. Lastly, the phenylthiourea analog 6 was synthesized by treating 2 with phenylisothiocyanate in methanol in 49% yield¹⁹. However, a thor-

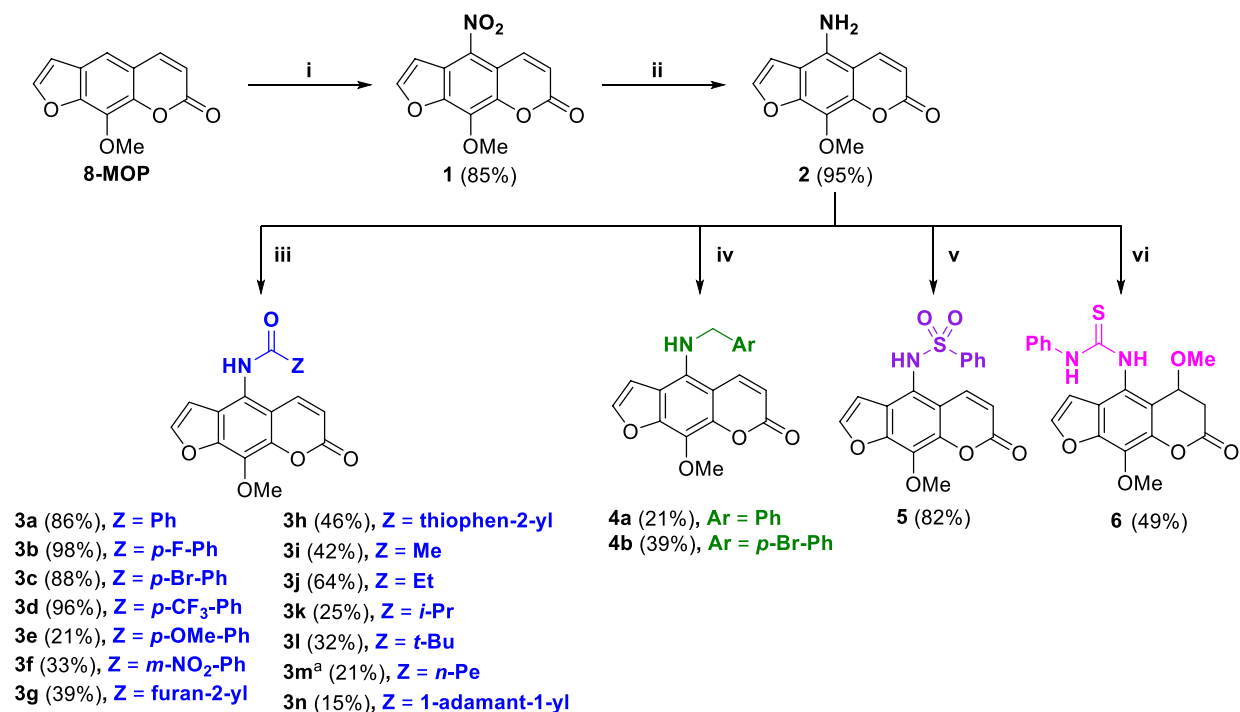


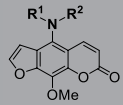
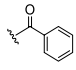
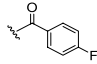
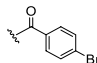
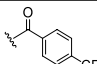
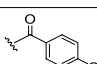
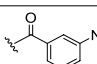
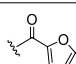
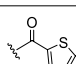
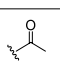
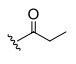
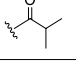
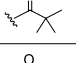
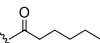
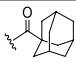
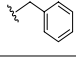
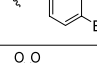
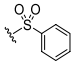
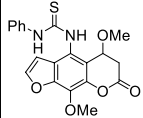
Figure 2. Synthesis of psoralen derivatives. (i) conc. HNO₃, CH₃COOH, rt; (ii) Sn (10.0 equiv.), 12 M HCl, EtOH, rt; (iii) acid chlorides (2.0–4.0 equiv.), K₂CO₃ (1.5 equiv.), DCM, rt or acetic anhydride (10.0 equiv.), K₂CO₃ (2.0 equiv.), pyridine (2.0 equiv.), cat. DMAP, DCM, rt; (iv) benzyl bromide (1.2–1.8 equiv.), K₂CO₃ (1.5 equiv.), acetone, 55 °C; (v) benzenesulfonyl chloride (1.1 equiv.), cat. DMAP, pyridine, 60 °C; (vi) phenylisothiocyanate (3.1 equiv.), MeOH, 65 °C; ^adisubstituted product.

ough characterization with ¹H, ¹³C, and HRMS revealed the lack of double bond on the coumarin part and the presence of a methoxy substituent at the C-6 position, which could be resulted from the nucleophilic Michael addition of MeOH used as the solvent.

Anti-breast cancer activity and cancer chemoprevention. Twenty of the synthesized psoralen derivatives were subjected to the evaluation of their cytotoxic effect against two breast cancer cell lines: MDA-MB-231 (hormone-independent) and T47-D (hormone-dependent), compared with three positive controls: doxorubicin, tamoxifen citrate, and lapatinib, via an MTT assay. Additionally, the cytotoxicity towards normal cells, human embryonal lung fibroblast cell MRC-5 was also assessed. Table 1 shows the %inhibition at the concentration of 50 µg mL⁻¹ and the IC₅₀ values after 48 h treatment of each compound without UVA irradiation. Almost all psoralen derivatives showed no cytotoxicity towards MRC-5, except only for **3f** with an IC₅₀ value of 77.33 µM, which was still less toxic than those of the three positive controls, implying their high safety profile. For the anti-cancer activity, most of the compounds exhibited modest cytotoxicity towards both cell lines, with the IC₅₀ of 10.14 µM for the most active compound against T47-D. We surmised that the cell lines used in our work were relatively less sensitive, as can be clearly observed for the adamantoyl derivative **3n** (**VIa**) with the IC₅₀ greater than 100 µM against MDA-MB-231, compared with the previously reported value (IC₅₀ = 2 µM)¹⁵. This lack of sensitivity of MDA-MB-231 was also observed for the positive control tamoxifen citrate whereby in our experiment exhibited much higher IC₅₀ value (IC₅₀ = 66.00 µM vs 1.6 µM)¹⁵. In fact, breast cancer cell lines could exhibit DNA alterations from the serial cultivation and cause phenotypical changes to cells resulting in variable sensitivities to drugs²⁰. Thus, in our case, the cancer cell lines used in this work could be more resistant than the previous report¹⁵.

Nevertheless, the cytotoxic results emphasize the importance of C-5 substituents in the anti-breast cancer activity of the synthesized psoralen derivatives. In general, the amide derivatives **3a–n** were relatively less active than the other series, with the benzamide derivatives (**3a–f**) exhibiting much greater cytotoxicity than the heteroaromatic (**3g–h**) and the aliphatic (**3i–n**) derivatives. Among the benzamide series, electron-withdrawing groups such as *p*-Br (**3c**), *p*-CF₃ (**3d**), and *m*-NO₂ (**3f**) showed better activity compared to other analogs. Likewise, the introduction of the *p*-Br in the benzyl amine analog **4b** also resulted in the increase in activity compared with the non-substituted analog **4a**. The sulfonamide (**5**) and thiourea (**6**) analogs were shown to inhibit breast cancer to some extent; however, the IC₅₀ were relatively high for both cell lines.

Comparing between the two breast cancer cell lines, the psoralen derivatives were less sensitive toward MDA-MB-231 cells with the best IC₅₀ values only at 71.01 µM from compounds **3f**. However, they appeared to exhibit good activity with T47-D and some of which exhibited the more potent IC₅₀ values than the positive drug tamoxifen citrate. This included compounds **3c**, **3d**, and **4b** with the IC₅₀ values of 10.14, 13.64, and

Comp.			Cytotoxic activity			Selectivity Index ^d (SI)	Aromatase inhibitory activity
	R ¹	R ²	MDA-MB-231 ^a	T47-D ^b	MRC-5 ^c		
8-MOP	-H		I (6%) ^e	I (16%) ^e	I (13%) ^e	-	I (21%) ^f
1	-NO ₂		I (39%) ^e	> 100	I (49%) ^e	> 1.2	I (34%) ^f
2	-NH ₂		I (3%) ^e	I (28%) ^e	I (5%) ^e	-	I (9%) ^f
3a	H		I (25%) ^e	I (45%) ^e	I (16%) ^e	-	I (3%) ^f
3b	H		I (34%) ^e	I (49%) ^e	I (11%) ^e	-	I (6%) ^f
3c	H		91.33 ± 7.84	10.14 ± 0.53	I (45%) ^e	> 11.9	I (13%) ^f
3d	H		I (35%) ^e	13.64 ± 0.26	I (41%) ^e	> 9.1	I (10%) ^f
3e	H		I (19%) ^e	I (38%) ^e	I (6%) ^e	-	I (15%) ^f
3f	H		71.01 ± 2.34	49.77 ± 0.50	77.33 ± 3.52	1.6	I (4%) ^f
3g	H		I (0.5%) ^e	I (24%) ^e	I (4%) ^e	-	I (16%) ^f
3h	H		I (8%) ^e	I (25%) ^e	I (3%) ^e	-	I (8%) ^f
3i	H		I (6%) ^e	I (20%) ^e	I (12%) ^e	-	I (7%) ^f
3j	H		I (3%) ^e	I (22%) ^e	I (4%) ^e	-	I (8%) ^f
3k	H		I (4%) ^e	I (36%) ^e	I (18%) ^e	-	I (8%) ^f
3l	H		I (1%) ^e	I (21%) ^e	I (6%) ^e	-	I (14%) ^f
3m			I (5%) ^e	I (15%) ^e	I (10%) ^e	-	9.4 ± 0.4
3n	H		> 100	43.06 ± 0.09	I (0%) ^e	> 3.0	I (5%) ^f
4a	H		> 100	31.12 ± 1.54	I (0%) ^e	> 5.0	I (46%) ^f
4b	H		94.35 ± 4.77	10.39 ± 0.79	I (0%) ^e	> 12.0	0.9 ± 0.2
5	H		I (36%) ^e	87.87 ± 6.34	I (9%) ^e	> 1.5	I (33%) ^f
6			91.86 ± 4.49	> 100	I (3%) ^e	> 1.2	I (18%) ^f
Doxorubicin			3.16 ± 0.26	1.46 ± 2.79	3.07 ± 0.22	2.1	-
Tamoxifen citrate			66.00 ± 2.48	20.86 ± 1.31	67.56 ± 10.50	3.2	-
Continued							

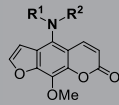
Comp.			Cytotoxic activity			Selectivity Index ^d (SI)	Aromatase inhibitory activity
	R ¹	R ²	MDA-MB-231 ^a	T47-D ^b	MRC-5 ^c		
Lapatinib			53.37 ± 0.31	9.78 ± 0.46	48.75 ± 9.45	5.0	–
Letrozole			–	–	–		2.6 ± 0.1 nM

Table 1. Cytotoxic and aromatase inhibitory activities (IC₅₀ [μM]) of psoralen derivatives. Results are obtained from three independent biological repeats; ^aHormone-independent breast cancer; ^bHormone-dependent breast cancer; ^cHuman embryonal lung fibroblast cell; ^dSelectivity Index (SI) = IC₅₀ for MRC-5/IC₅₀ for T47-D; ^e%Inhibition at the concentration of 50 mg mL⁻¹; ^f%Inhibition at the concentration of 12.5 μM; I = %inhibition lower than 50% at a specified concentration; – not determined.

10.39 μM, respectively. Gratifyingly, these three derivatives also presented high selectivity. The derivatives **3c**, **3d**, and **4b** had selectivity index (SI) with T47-D more than 11.9, 9.08, and 12.0, which were at least ca. 6.7, 2.8 and 3.7-fold superior to that of tamoxifen citrate (SI = 3.23), the current approved therapeutic drug for estrogen positive breast cancer.

Estrogens are the critical risk factor for breast cancer initiation and progression and the aromatase enzyme involves in the final step conversion of androgens to estrogens^{21,22}. As more than 70% of all breast cancers are classified as ER+ (estrogen receptor positive) and estrogen dependent, identification of compounds that can interfere this molecular mechanism could be clinically useful for management of hormone dependent breast cancer. In this study, the synthesized psoralen derivatives were also tested for aromatase inhibitory activity (AIA) which is considered to be one of chemopreventive mechanisms for hormone dependent breast cancer. According to Table 1, although only compounds **3m** and **4b** exhibited anti-aromatase activity, both of them possessed very high efficacy with the IC₅₀ values of 9.4 and 0.9 μM, respectively. Further analysis to find any correlation between the cytotoxicity of the hormone dependent breast cancer T47-D and anti-aromatase activity revealed that, even though the tertiary amide **3m** has good chemopreventive activity in AIA with the IC₅₀ = 9.4 μM, it has no anti-cancer activity. Moreover, the compounds with good anti-breast cancer activity such as **3c** and **3d**, even so, showed no chemopreventive activity in AIA. Hence, it might be said that the inhibition of aromatase enzyme and anti-breast cancer activity in T47-D cells were not necessarily correlated. Nevertheless, secondary amine **4b** was highly potent in both anti-breast cancer activities (cytotoxic activity in T47-D cells, IC₅₀ = 10.39 μM and chemo-preventive activity in AIA, IC₅₀ = 0.9 μM). As the preferable concurrent cytotoxic and aromatase inhibitory activities could provide synergistic potential for management of estrogen-dependent breast cancer, the structure of bromobenzyl amine **4b** is particularly promising for further study to improve anti-cancer activity and further elucidate the mechanism.

Psoralen derivatives have been reported to be associated with various aromatase and estrogen related events. For example, administer of 5-MOP (bergapten) and 8-MOP to female rats significantly reduced circulating estrogen levels in a dose-dependent manner²³. 8-MOP decreased both the amount of aromatase protein in the ovary and the level of circulating estradiol in female Wistar rats²⁴. Bergapten reduced the levels of estrogen receptor in MCF-7 breast cancer cells as well as in the tamoxifen-resistant clone²⁵. In the in-vitro ERα antagonist potential, xanthotoxol, bergapten, angelicin, psoralen and isoimperatorin antagonized ETRα activity in MCF-7 cells with IC₅₀ values of 0.7, 1.2, 11.0, 24.1 and 54.3 μM, respectively²⁶. On estrogens and growth factor signaling in breast cancer, psoralens may act by inhibiting aromatase enzyme, metalloproteinases (MMPs) and CYP enzymes⁶. However, to date, the supporting evidence on a role of psoralens as an aromatase inhibitor is quite elusive. The results from this work revealed some psoralen derivatives that could exert aromatase inhibitory activity, thus this finding could be initial point for further investigation to the more potent aromatase inhibitor. Additionally, as psoralens have been reported to be related to several anti-breast cancer mechanistic pathways⁶, targeting multiple pathways by psoralens which could promote synergistic effects for cancer treatment is worth to be explored.

Apart from anti-aromatase activity, all psoralen derivatives were also evaluated in several chemopreventive assays that represented different defense mechanisms against cancer, including radical scavenging of 1,1-diphenyl-2-picrylhydrazyl (DPPH) assay, inhibition of superoxide formation by inhibiting xanthine oxidase (IXO), antioxidant properties by scavenging of superoxide anion radical generation induced by 12-O-tetradecanoylphorbol-13-acetate (TPA) in differentiated HL-60 human promyelocytic leukemia cells (HL-60 antiox.) and by reaction of xanthine/xanthine oxidase (XXO), anti-inflammatory by inhibition of lipoxygenase (LOX). The results showed that the majority of compounds had low to moderate chemopreventive activities (see Supplementary Table S1).

Phototoxicity. All the synthesized compounds, and a positive control lapatinib were first preliminarily tested for their cytotoxicity towards an HER2+ breast cancer cells, SK-BR-3, both in the absence and the presence of UVA irradiation (2.0 J cm⁻²) as shown in Fig. 3.

Strikingly, the cytotoxicity towards SK-BR-3 for most of the psoralen derivatives were immensely enhanced by the UVA irradiation, except for the parent 8-MOP, which showed little to no activity neither in the absence nor the presence of UV light. In contrast with the results of MDA-MB-231 and T47-D (Table 1), the amide derivatives

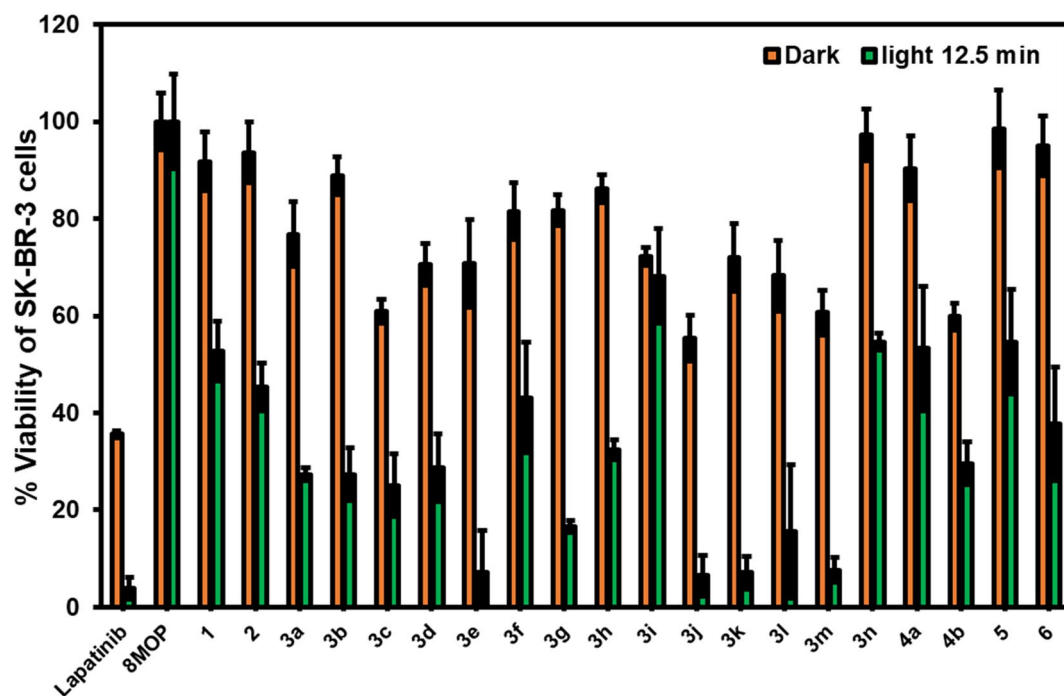


Figure 3. Dark and light-activated cytotoxicity of psoralen derivatives against SK-BR-3 at the concentration of 50 μM ; orange bar = %viability in the dark, green bar = %viability under irradiation with UVA (2.0 J cm^{-2}).

Comp	IC_{50} (μM) dark		IC_{50} (μM) with UVA ^a	
	SK-BR-3 ^b	MDA-MB-231 ^c	SK-BR-3 ^b	MDA-MB-231 ^c
8-MOP	> 100	> 100	24.66 \pm 3.02	> 100
3e	> 100	> 100	66.72 \pm 2.75	> 100
3g	> 100	> 100	2.71 \pm 0.84	> 100
3j	> 100	> 100	3.05 \pm 1.02	> 100
3k	> 100	> 100	66.09 \pm 5.21	> 100
3l	> 100	> 100	48.14 \pm 3.07	> 100
3m	> 100	> 100	27.09 \pm 1.20	> 100
Lapatinib	25.27 \pm 0.99	73.00 \pm 2.53	0.16 \pm 0.03	8.60 \pm 0.82

Table 2. Dark and light-activated cytotoxicity of psoralen derivatives against breast cancer cells. Results are obtained from three independent biological repeats; ^aIrradiation with UVA (2.0 J cm^{-2}); ^bHER2+ breast cancer; ^cHER2- breast cancer.

3a–n exhibited slightly greater dark cytotoxicity against the SK-BR-3, compared with the amine, sulfonamide, and thiourea derivatives. Notably, the UVA irradiation enhanced the cytotoxicity of the furanyl (**3g**) and aliphatic amides (**3j–m**) to a much greater extent than those with aromatic or thiophene rings. Furthermore, the size of the aliphatic substituent contributed greatly to the phototoxicity: the compound bearing a small acetyl (**3i**) or very bulky adamantoyl (**3n**) groups were found to produce relatively higher %viability of the cancer cells. In addition, the benzamide derivative bearing an electron-donating *p*-OMe (**3e**) also showed very promising anti-cancer activity. In this regard, we selected the compounds that gave the %viability under UVA irradiation lower than 20% for further investigation. The selected compounds were screened for their IC_{50} values against both HER2+ breast cancer (SK-BR-3), and HER2- breast cancer (MDA-MB-231) in both dark and light-activated conditions (Table 2). Additionally, a negative control study was also performed with SK-BR-3 and MDA-MB-231 cells in the absence of tested compound under UVA irradiation (See Fig S7., Supporting Information). The % cell viability of >85% of both SK-BR-3 and MDA-MB-231 cells after UVA irradiation suggested that the UVA radiation exhibited marginal significant effect toward both cell lines.

In the experiment with the tested compounds, all the compounds were found to be inactive against both cancer cells in the absence of UV irradiation. However, a stark contrast in the phototoxicity between the two cell lines was observed. For SK-BR-3, the selected psoralen derivatives exhibited moderate to exceptional phototoxicity with the IC_{50} ranging from 2.71 to 66.72 μM . In contrast, no phototoxicity was observed for all derivatives against MDA-MB-231, which is in consistent with the previously reported finding by Xia and co-workers, suggesting that these psoralen derivatives may exert phototoxicity via the mechanism involving the interaction

with HER2¹¹. To our surprise, the most active compound was found to be the amide analog **3g** bearing a furanyl group, giving the IC₅₀ of 2.71 μM which is almost tenfold increase from the parent 8-MOP.

It is worth mentioning that in contrast to the psoralen derivatives, the strong phototoxicity of a positive control lapatinib could be clearly observed in both SK-BR-3 and MDA-MB-231. Since the selective phototoxicity activity of 8-MOP towards HER2+ breast cancer has been proposed to associate with the catalytic autokinase domain of the HER2¹¹, while it is well-known that lapatinib binds to the ATP-binding sites of both HER1 and HER2²⁷. Therefore, it is conceivable that the strong phototoxicity of lapatinib might involve other mechanisms of action as the activity could be found in both HER2+ and HER2- breast cancer cell lines. It should also be noted that lapatinib had an anti-cancer activity even without UVA irradiation (Table 2) and had significant toxicity towards normal cells (Table 1), hence resulting in a limited selectivity. Consequently, the PUVA phototherapy with these psoralen derivatives could provide a unique selectivity not only towards the breast cancer cells, but also in the area of the biological action, which could be valuable for potential targeted therapy. Nevertheless, it should also take caution that both lapanib and the parent 8-MOP are known to have phototoxic potential as determined by 3T3 NRU assay^{28,29}; therefore, the cutaneous adverse effects associated with these compounds is necessary to be identified. Additionally, mitigation of the adverse effects of UVA by using therapeutic approach such as X-PACT (X-ray Psoralen Activated Cancer Therapy)³⁰, should be worthwhile considered in the development of psoralen derivatives as breast cancer targeted therapy.

Molecular docking studies. The mechanism in which psoralens can inhibit breast cancer cells with UVA irradiation have been reported via multiple pathways, such as through DNA intercalation and inhibition of HER2¹¹. From our study, the difference in the phototoxicity between MDA-MB-231 and SK-BR-3 demonstrated by our newly synthesized psoralen derivatives strongly suggests HER2 as a plausible target. In order to analyze the molecular binding between the psoralen derivatives and HER2, we performed molecular docking study between all seven ligands in Table 2 against HER2 using Autodock Vina (Supplementary Table S2). The docking results of three representative ligands 8-MOP (parent ligand, IC₅₀ = 24.66 μM), **3g** (the most active, IC₅₀ = 2.71 μM) and **3j** (the second most active, IC₅₀ = 3.05 μM) docked poses and docking scores of the corresponding ligands are shown in Fig. 4.

As shown in Fig. 4, HER2 can suitably accommodate all the psoralen ligands in the same binding pocket. This result is coherent with the work by Xia et al., reporting that psoralen derivative was bound to the HER2 at the aa 861–868 and aa 869–883 regions, albeit upon UVA irradiation¹¹. The docking scores of ligands, 8-MOP, **3g**, and **3j** are -7.9, -9.4 and -8.3 kcal mol⁻¹, respectively. A less negative molecular docking score of 8-MOP suggests less favorable interactions between the predicted pose of 8-MOP with the HER2 binding site, compared to **3g**, and **3j**. Both **3g** and **3j** docked poses revealed hydrogen-bonds with Met801 residue (2.2 and 2.7 Å) and with ASP863 (2.4 Å). Notably, the hydrogen bonds with Met801 residue are also seen in the co-crystallized inhibitor as reported by Aertgeerts et al.³¹. Therefore, these favorable interactions of **3g** and **3j** at the active site of HER2 could be a reason that contributes towards the exceptional phototoxicity and selectivity of these derivatives against the HER2-overexpressing breast cancer cells.

Cell morphology. To clarify their anti-proliferative effects, the morphology of SK-BR-3 cells treated with different concentrations of compounds **3g**, **3j**, and lapatinib under dark and light activation was observed using a light microscope. Notably, the difference of cell morphology between dark and light activation of the **3g** and **3j**-treated SK-BR-3 cells could be clearly presented (Fig. 5). The cells under dark condition maintained morphology of intact cells after treatment at 48 h, while under light activation using UVA 2.0 J cm⁻², the morphology of treated SK-BR-3 cells was significantly changed. These results were in agreement with the cytotoxicity results whereby the cytotoxic activity of the **3g** and **3j**-treated SKBR-3 cells could be observed only under UVA irradiation (Table 2). Furthermore, the increase in the apoptotic index, which is characterized by the features such as cell shrinkage, plasma membrane blebbing, and cell disintegration into apoptotic bodies, was presented in a dose dependent manner in both the **3g**- and **3j**-treated SK-BR-3 cells. At higher concentrations (10, 20 or 50 μM), the cells were almost completely broken down, while at lower concentrations (1, 2.5, or 5 μM), varying degrees of cell shrinkage and membrane blebbing were still depicted. For lapatinib, in contrast to **3g** and **3j**, the morphological changes indicating apoptosis of the treated cells were depicted under both dark and light activation in a dose dependent manner. Nevertheless, the higher degree of apoptotic index was detected under light activation.

Based on these finding, the significant inhibition of SK-BR-3 cells under UVA irradiation of **3g** and **3j** appeared to be related to induction of cell apoptosis, which is corresponding to the previous report regarding the ability PUVA to block HER2 signaling and induce tumor cell apoptosis¹¹. However, the apoptosis induced by lapatinib may involve in different mechanism as dissimilar results could be observed.

The predicted physicochemical properties. In order to evaluate the druggability of the compounds, the physicochemical properties and analysis by Lipinski's rule of five were conducted using SwissADME website service. All the calculated parameters are presented in Table 3. Although the introduction of the C-5 substituents generally leads to an increase in the TPSA, the values remain less than 140 Å². Combining with the number of rotatable bonds of less than 10, this suggests that the compounds might exhibit good oral bioavailability³². Moreover, the increase in the lipophilicity for these derivatives also benefits cell permeability³³. However, these derivatives suffer from a slight decrease in the aqueous solubility; nevertheless, based on Log S, these derivatives are categorized within the "soluble" or "moderately soluble" classes, which are sufficient to be used as a drug³⁴. For example, the aqueous solubility of the most active compound, **3g**, was predicted to be 182 μM, which is well above its working concentration (IC₅₀ with UVA = 2.71 μM against SK-BR-3). Finally, no violation of Lipinski's

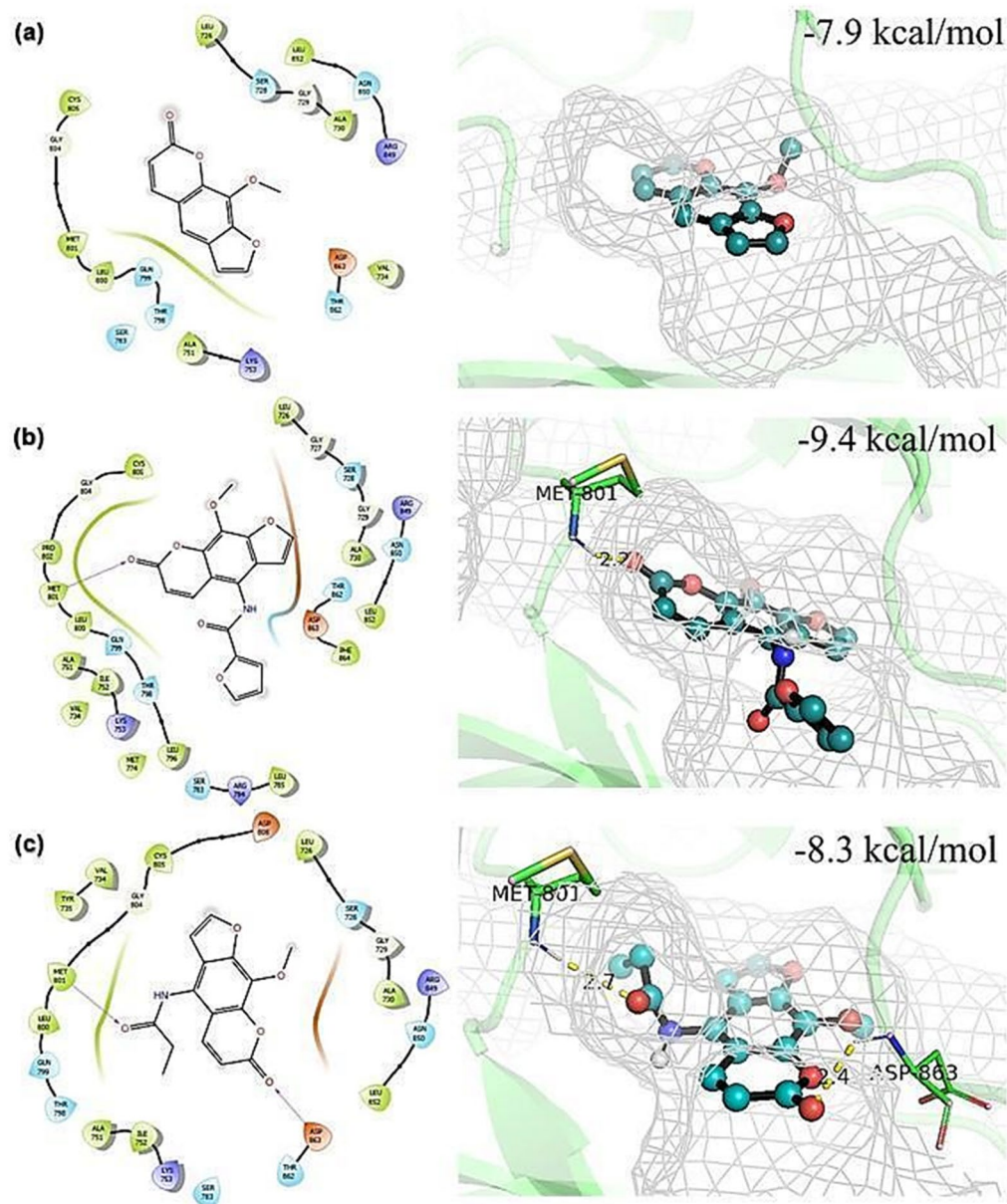


Figure 4. 2D and 3D representations of top-scoring poses obtained from molecular docking models between psoralen derivatives: 8-MOP (a), **3g** (b), or **3j** (c) and HER2 (PDB code: 3PP0)^{44,45}. The purple arrows represent the hydrogen bonding. Ligand molecules shown as ball and stick models are colored cyan (carbon), red (oxygen), blue (nitrogen), and white (polar hydrogen). Hydrogen bonding is shown in yellow dashed lines to amino acid residues, and the distance (Å) between atoms of amino acids and ligand is displayed.

rule of five was observed for all the compounds as the molecular weight, the number of hydrogen bond acceptors and donors, and the lipophilicity are all within the acceptable limits³⁵.

Materials and methods

Synthesis and identification of psoralen derivatives. All reagents and solvents were obtained from Sigma-Aldrich (St. Louis, MO, USA), TCI Chemicals (Tokyo, Japan), Fluorochem (Hadfield, Derbyshire, UK) and Merck (Darmstadt, Germany). All solvents for column chromatography from RCI Labscan (Samutsakorn, Thailand) were distilled before use. ¹H, ¹³C and ¹⁹F NMR spectra were recorded on Bruker Avance (400, 101 and 376 MHz) and Jeol Avance (500 and 126 MHz). Chemical shifts are reported as δ values in parts per million (ppm) relative to tetramethylsilane (δ 0.00) or the solvent residue in DMSO-*d*₆ (δ 2.50) or CDCl₃ (δ 7.26). Data are reported as follows; chemical shift (multiplicity, coupling constants in Hz, integrate intensity, assignment). Abbreviations of multiplicity were as follows; s: singlet, d: doublet, t: triplet, q: quartet, m: multiplet, br: broad. Chemical shifts for ¹³C NMR are reported as δ values in parts per million (ppm) relative to DMSO-*d*₆.

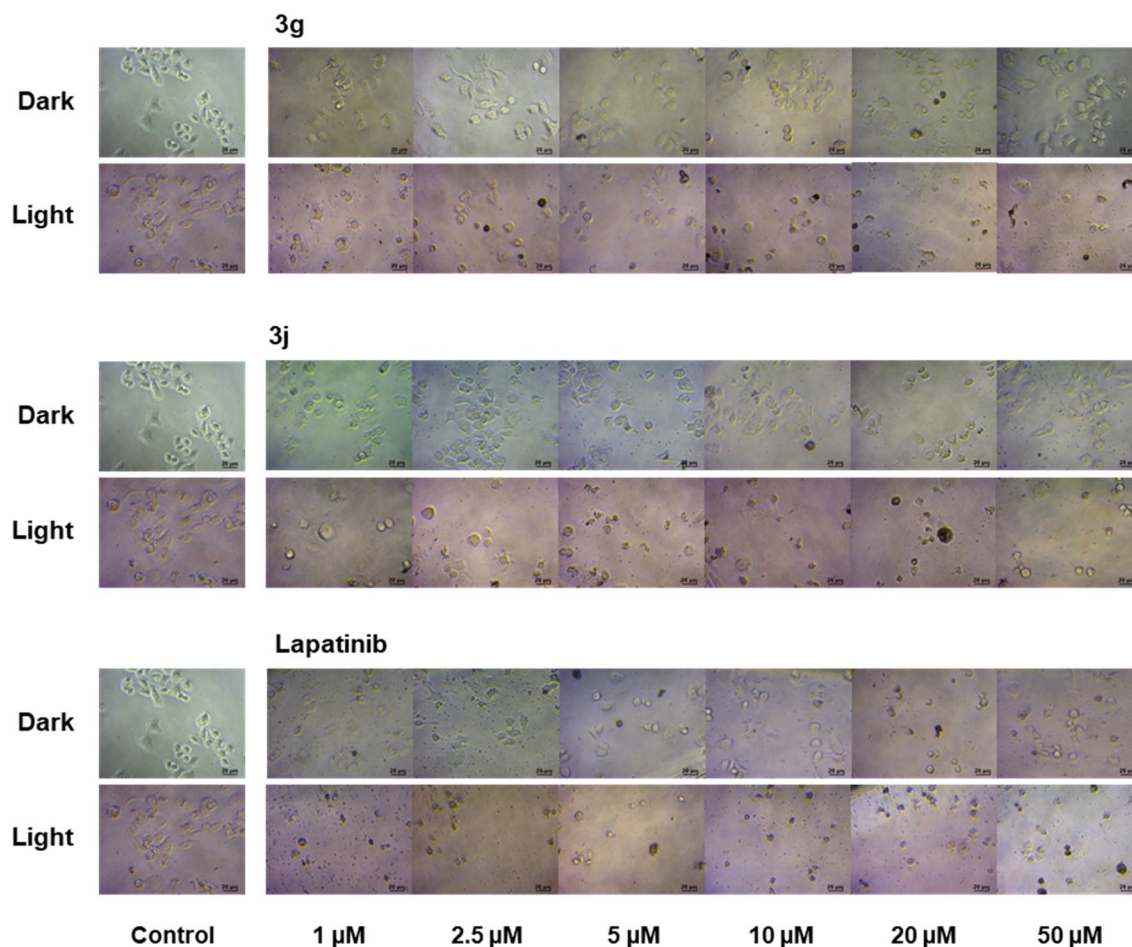


Figure 5. The morphology of SK-BR-3 cells treated with different concentrations of compounds **3g**, **3j**, and lapatinib at 48 h under dark and light activation (irradiation with UVA 2.0 J/cm²). Cells treated with 1% DMSO served as controls.

(δ 39.52) and CDCl₃ (δ 77.16) as internal standard. High-resolution mass spectra (HRMS) data were obtained with micro-TOF mass spectrometer. IR spectra were recorded using the Thermo Scientific Nicolet iS50 FTIR spectrometer with ATR module and are reported in wave number (cm⁻¹). Reactions were monitored by thin-layer chromatography (TLC) using aluminium Merck TLC plates coated with silica gel 60 F254. The reactions were monitored by TLC (ethyl acetate:hexanes, 1:1, 1:2, 1:3, 2:3, 1:4, 1:9, 100%DCM, and DCM:MeOH, 95:5 v/v). Normal phase column chromatography was performed using silica gel 60 (0.063–0.200 mm, 70–230 mesh ASTM, Merck, Darmstadt, Germany). Melting points were measured using a melting point apparatus (Griffin) and are uncorrected.

9-Methoxy-4-nitro-7H-furo[3,2-g]chromen-7-one (1). The title compound was synthesized using a slightly modified literature procedure using 8-MOP (2.20 g, 10.00 mmol) in glacial acetic acid (21.0 mL), and conc. HNO₃ (17.1 mL)¹⁶. The precipitate was collected and washed with DI water to give the title compound. Yellow solid; 85% yield; **Mp**: 237–238 °C; **HPLC**: 99.11% purity; **TLC** (100%DCM): R_f=0.45; **¹H NMR** (400 MHz, CDCl₃): δ 8.78 (d, *J*=10.2 Hz, 1H), 7.86 (d, *J*=2.3 Hz, 1H), 7.42 (d, *J*=2.3 Hz, 1H), 6.63 (d, *J*=10.2 Hz, 1H), 4.49 (s, 3H); **¹³C NMR** (101 MHz, CDCl₃): δ 165.1, 158.5, 157.7, 149.6, 145.3, 145.1, 139.4, 124.7, 118.8, 112.4, 107.6, 61.7; **IR** (neat): 3156 (C–H), 1736 (C=O), 1571 (C=C), 1497 (N=O), 1314 (N=O), 1282 (C–O), 1265 (C–O) cm⁻¹; Data are consistent with literature values³⁶.

4-Amino-9-methoxy-7H-furo[3,2-g]chromen-7-one (2). The title compound was synthesized using a slightly modified literature procedure using **1** (2.09 g, 8.00 mmol) in methanol (15.0 mL), tin powder (3.80 g, 40.00 mmol), and conc. hydrochloric acid (40.0 mL)¹⁷. The precipitate was collected and washed with hexanes to give the title compound. Green solid; 95% yield; **Mp**: 238–239 °C; **HPLC**: 98.12% purity; **TLC** (DCM:MeOH, 95:5 v/v): R_f=0.60; **¹H NMR** (500 MHz, DMSO-*d*₆): δ 8.32 (d, *J*=9.8 Hz, 1H), 7.85 (d, *J*=2.2 Hz, 1H), 7.20 (d, *J*=2.2 Hz, 1H), 6.49 (br s, 2H), 6.12 (d, *J*=9.8 Hz, 1H), 3.90 (s, 3H); **¹³C NMR** (126 MHz, DMSO-*d*₆): δ 160.8, 150.5, 145.0, 144.7, 141.5, 136.6, 123.4, 111.7, 108.6, 106.2, 100.5, 61.7; **IR** (neat): 3478 (N–H), 3383 (N–H), 3137 (C–H), 3107 (C=C), 2957 (C–H), 1701 (C=O), 1647 (N–H), 1587 (C=C), 1480 (C=C), 1446 (C=C), 1050 (C–O)

Comp.	MW	Fraction Csp ³ ^a	Rotatable bonds	HBA ^b	HBD ^c	TPSA ^d	MLOGP ^e	ESOL Log S ^f	Lipinski #violations ^g
8-MOP	216.19	0.08	1	4	0	52.58	1.18	-2.98	0
1	261.19	0.08	2	6	0	98.4	0.21	-2.99	0
2	231.21	0.08	1	4	1	78.6	0.61	-2.6	0
3a	335.31	0.05	4	5	1	81.68	1.94	-4.18	0
3b	353.31	0.05	4	6	1	81.68	2.32	-4.34	0
3c	414.21	0.05	4	5	1	81.68	2.55	-5.09	0
3d	403.31	0.1	5	8	1	81.68	2.5	-5.02	0
3e	365.34	0.1	5	6	1	90.91	1.63	-4.24	0
3f	380.31	0.05	5	7	1	127.5	1.06	-4.23	0
3g	325.27	0.06	4	6	1	94.82	0.7	-3.74	0
3h	341.34	0.06	4	5	1	109.92	1.5	-4.22	0
3i	273.24	0.14	3	5	1	81.68	0.67	-2.56	0
3j	287.27	0.2	4	5	1	81.68	0.92	-3.03	0
3k	301.29	0.25	4	5	1	81.68	1.17	-3.46	0
3l	315.32	0.29	4	5	1	81.68	1.42	-3.75	0
3m	427.49	0.46	12	6	0	89.96	2.51	-5.32	0
3n	393.43	0.48	4	5	1	81.68	2.77	-4.89	0
4a	321.33	0.11	4	4	1	64.61	2.15	-4.52	0
4b	400.22	0.11	4	4	1	64.61	2.76	-5.42	0
5	371.36	0.06	4	6	1	107.13	1.24	-4.19	0
6	398.43	0.2	6	5	2	114.05	1.55	-3.95	0

Table 3. Predicted physicochemical properties of psoralen derivatives^{46,47}. ^aThe ratio of *sp*³ hybridized carbons over the total carbon count of the molecule; ^bhydrogen bond acceptor; ^chydrogen bond donor; ^dtopological polar surface area [Å²]; ^elipophilicity: Moriguchi octanol–water partition coefficient (MLOGP) is based on quantitative structure–logP relationships, by using topological indexes; ^flog of the aqueous solubility measured in mol L⁻¹, according to the Estimating Aqueous Solubility (ESOL); ^gLipinski's rule of five (MW ≤ 500, MLogP ≤ 4.15, HBA ≤ 10, and HBD ≤ 5).

cm⁻¹; **HRMS** (ESI⁺): *m/z* calcd for C₁₂H₉NO₄Na⁺ [M+Na]⁺ 254.0429, found 254.0428. Data are consistent with literature values³⁶.

General procedure for the synthesis of 3a–n¹⁵. To a solution of **2** in DCM was added the corresponding acid chloride (4.0 equiv.) and K₂CO₃ (1.5 equiv.) at room temperature. The reaction mixture was refluxed overnight. Upon completion, the reaction mixture was quenched with DI water. The resulting mixture was neutralized by sat. NaHCO₃ and extracted with EtOAc (3 times). The combined organic layers were washed with brine, dried, filtered, then concentrated in vacuo to give the amide derivatives.

***N*-(9-Methoxy-7-oxo-7H-furo[3,2-*g*]chromen-4-yl)benzamide (3a).** The crude product was purified by silica gel column chromatography (eluent: EtOAc:hexanes = 1:9–1:1) to provide the title compound. Off-white solid; 86% yield; **Mp**: 220–222 °C; **HPLC**: 98.67% purity; **TLC** (EtOAc:hexanes, 1:1): *R*_f = 0.67; **¹H NMR** (400 MHz, DMSO-*d*₆): δ 10.60 (br s, 1H), 8.09–7.99 (m, 4H), 7.61 (d, *J* = 7.5 Hz, 1H), 7.54 (t, *J* = 7.5 Hz, 2H), 6.92 (d, *J* = 2.3 Hz, 1H), 6.41 (d, *J* = 9.8 Hz, 1H), 4.16 (s, 3H); **¹³C NMR** (101 MHz, DMSO-*d*₆): δ 166.4, 159.6, 147.4, 147.2, 142.9, 141.7, 133.9, 132.2, 130.8, 128.7, 128.2, 123.8, 121.8, 113.9, 112.9, 106.5, 6.4; **IR** (neat): 3235 (N–H), 3060 (C–H), 2944 (C–H), 1726 (C=O), 1647 (C=O), 1593 (C=C), 1145 (C–O) cm⁻¹; **HRMS** (ESI⁺): *m/z* calcd for C₁₉H₁₃NO₅Na⁺ [M+Na]⁺ 358.0686, found 358.0681.

4-Fluoro-*N*-(9-methoxy-7-oxo-7H-furo[3,2-*g*]chromen-4-yl)benzamide (3b). The crude product was washed with hexanes to give the title compound. Gray solid; 98% yield; **Mp**: 276–277 °C; **HPLC**: 98.91% purity; **TLC** (EtOAc:hexanes, 1:1): *R*_f = 0.60; **¹H NMR** (400 MHz, DMSO-*d*₆): δ 10.60 (br s, 1H), 8.11 (dd, *J* = 8.5, 5.4 Hz, 2H), 8.05 (d, *J* = 2.3 Hz, 1H), 8.02 (d, *J* = 9.8 Hz, 1H), 7.36 (t, *J* = 8.6 Hz, 2H), 6.90 (d, *J* = 2.3 Hz, 1H), 6.39 (d, *J* = 9.7 Hz, 1H), 4.14 (s, 3H); **¹³C NMR** (101 MHz, DMSO-*d*₆): δ 166.0, 165.6, 159.9, 147.7, 147.4, 143.1, 141.9, 131.2 (d, *J* = 9.3 Hz), 130.6 (d, *J* = 2.9 Hz), 124.1, 121.8, 115.9, 115.7, 114.2, 113.2, 106.7, 61.6; **¹⁹F NMR** (376 MHz, DMSO-*d*₆): δ -108.20 (tt, *J* = 8.6, 3.2 Hz); **IR** (neat): 3395 (N–H), 3163 (C–H), 2950 (C–H), 1725 (C=O), 1674 (C=O), 1592 (C=C), 1475 (N–H), 1257 (C–O), 1168 (C–O), 1139 (C–O), 748 (C–F) cm⁻¹; **HRMS** (ESI⁺): *m/z* calcd for C₁₉H₁₂FNO₅Na⁺ [M+Na]⁺ 376.0597, found 376.0590.

4-Bromo-*N*-(9-methoxy-7-oxo-7H-furo[3,2-*g*]chromen-4-yl)benzamide (3c). The crude product was purified by silica gel column chromatography (eluent: DCM:MeOH = 100:0 to 97:3 v/v) to provide the title compound. Gray solid; 88% yield; **Mp**: 293–294 °C; **HPLC**: 98.12% purity; **TLC** (DCM:MeOH, 95:5 v/v): *R*_f = 0.42; **¹H NMR**

(400 MHz, DMSO- d_6): δ 10.56 (br s, 1H), 7.93 (d, $J=2.2$ Hz, 1H), 7.90 (d, $J=9.8$ Hz, 1H), 7.85 (d, $J=8.5$ Hz, 2H), 7.62 (d, $J=8.5$ Hz, 2H), 6.78 (d, $J=2.2$ Hz, 1H), 6.28 (d, $J=9.8$ Hz, 1H), 4.02 (s, 3H); $^{13}\text{C NMR}$ (126 MHz, DMSO- d_6): δ 166.0, 160.0, 147.8, 147.4, 143.1, 142.0, 137.8, 133.3, 132.0, 131.2, 130.6, 126.3, 124.1, 121.7, 114.3, 113.2, 106.8, 61.7; **IR** (neat): 3211 (N-H), 3149 (C-H), 2924 (C-H), 1734 (C=O), 1647 (C=O), 1590 (N-H), 1142 (C-O), 1116 (C-O), 752 (C-Br) cm^{-1} ; **HRMS** (ESI $^+$): m/z calcd for $\text{C}_{19}\text{H}_{12}\text{BrNO}_5\text{Na}^+$ $[\text{M}+\text{Na}]^+$ 437.9776, found 437.9762.

***N*-(9-Methoxy-7-oxo-7H-furo[3,2-g]chromen-4-yl)-4-(trifluoromethyl)benzamide (3d)**. The crude product was washed with hexanes to give the title compound. Off-white solid; 96% yield; **Mp**: 284–286 °C; **HPLC**: 96.30% purity; **TLC** (EtOAc:hexanes, 1:1): $R_f=0.50$; $^1\text{H NMR}$ (400 MHz, DMSO- d_6): δ 10.78 (br s, 1H), 8.20 (d, $J=8.0$ Hz, 2H), 8.08–8.00 (m, 2H), 7.88 (d, $J=8.1$ Hz, 2H), 6.90 (d, $J=2.3$ Hz, 1H), 6.38 (d, $J=9.9$ Hz, 1H), 4.12 (s, 3H); $^{13}\text{C NMR}$ (101 MHz, DMSO- d_6): δ 165.4, 159.6, 147.6, 147.2, 142.9, 141.6, 137.8, 132.0 (q, $J=32.0$ Hz), 131.0, 129.2, 125.7 (q, $J=4.1$ Hz), 124.1 (q, $J=271.7$ Hz), 123.9, 121.2, 114.1, 113.0, 106.5, 61.4; $^{19}\text{F NMR}$ (376 MHz, DMSO- d_6): δ -61.34 (s, 3F); **IR** (neat): 3230 (N-H), 3123 (C-H), 2945 (C-H), 1724 (C=O), 1652 (C=O), 1590 (C=C), 1521 (N-H), 1145 (C-O), 1108 (C-O), 824 (C-F) cm^{-1} ; **HRMS** (ESI $^+$): m/z calcd for $\text{C}_{20}\text{H}_{12}\text{F}_3\text{NO}_5\text{Na}^+$ $[\text{M}+\text{Na}]^+$ 426.0565, found 426.0570.

4-Methoxy-*N*-(9-methoxy-7-oxo-7H-furo[3,2-g]chromen-4-yl)benzamide (3e). The crude product was purified by silica gel column chromatography (eluent: EtOAc:hexanes=1:9–1:1) to provide the title compound. White solid; 31% yield; **Mp**: 211–212 °C; **HPLC**: 98.31% purity; **TLC** (EtOAc:hexanes, 4:1): $R_f=0.40$; $^1\text{H NMR}$ (500 MHz, DMSO- d_6): δ 10.44 (br s, 1H), 8.05 (d, $J=2.3$ Hz, 1H), 8.03 (d, $J=8.8$ Hz, 2H), 7.99 (d, $J=9.9$ Hz, 1H), 7.06 (d, $J=8.8$ Hz, 2H), 6.88 (d, $J=2.1$ Hz, 1H), 6.40 (d, $J=9.8$ Hz, 1H), 4.15 (s, 3H), 3.82 (s, 3H); $^{13}\text{C NMR}$ (126 MHz, DMSO- d_6): δ 166.0, 162.7, 159.9, 147.6, 147.4, 143.1, 142.0, 130.9, 130.4, 126.1, 124.0, 122.3, 114.1, 114.0, 113.1, 106.8, 61.6, 55.9; **IR** (neat): 3214 (N-H), 3128 (C-H), 2950 (C-H), 1725 (C=O), 1644 (C=O), 1607 (C=C), 1592 (N-H), 1498 (C=C), 1478 (C=C), 1254 (C-O), 1023 (C-O) cm^{-1} ; **HRMS** (ESI $^+$): m/z calcd for $\text{C}_{24}\text{H}_{29}\text{NO}_6\text{Na}^+$ $[\text{M}+\text{Na}]^+$ 388.0797, found 388.0804.

***N*-(9-Methoxy-7-oxo-7H-furo[3,2-g]chromen-4-yl)-3-nitrobenzamide (3f)**. The crude product was purified by silica gel column chromatography (eluent: EtOAc:hexanes=2:3–2:1) and then recrystallized with acetone to provide the title compound. Yellow solid; 33% yield; **Mp**: 267–268 °C; **HPLC**: 99.21% purity; **TLC** (EtOAc:hexanes, 1:2): $R_f=0.59$; $^1\text{H NMR}$ (500 MHz, DMSO- d_6): δ 10.88 (br s, 1H), 8.81 (s, 1H), 8.42–8.35 (m, 2H), 8.04 (d, $J=9.9$ Hz, 1H), 8.00 (d, $J=2.2$ Hz, 1H), 7.77 (t, $J=8.0$ Hz, 1H), 6.89 (d, $J=2.2$ Hz, 1H), 6.35 (d, $J=9.9$ Hz, 1H), 4.09 (s, 3H); $^{13}\text{C NMR}$ (126 MHz, DMSO- d_6): δ 164.8, 160.0, 148.3, 147.9, 147.4, 143.2, 142.0, 135.8, 135.0, 131.3, 130.8, 127.0, 124.1, 123.4, 121.4, 114.4, 113.2, 106.9, 61.7; **IR** (neat): 3236 (N-H), 3117 (C-H), 1720 (C=O), 1660 (C=C), 1520 (N-O), 1350 (N-H) cm^{-1} ; **HRMS** (ESI $^+$): m/z calcd for $\text{C}_{19}\text{H}_{12}\text{N}_2\text{O}_7\text{H}^+$ $[\text{M}+\text{H}]^+$ 381.0767, found 381.0817.

***N*-(9-Methoxy-7-oxo-7H-furo[3,2-g]chromen-4-yl)furan-2-carboxamide (3g)**. The crude product was purified by silica gel column chromatography (eluent: DCM:MeOH=100:0 to 99:1 v/v) to provide the title compound. Yellow-green solid; 39% yield; **Mp**: 227–228 °C; **HPLC**: 99.45% purity; **TLC** (DCM:MeOH, 95:5 v/v): $R_f=0.64$; $^1\text{H NMR}$ (500 MHz, DMSO- d_6): δ 10.52 (br s, 1H), 7.97 (d, $J=2.3$ Hz, 1H), 7.93–7.85 (m, 2H), 7.28 (d, $J=3.4$ Hz, 1H), 6.79 (d, $J=2.3$ Hz, 1H), 6.63 (dd, $J=3.6, 1.8$ Hz, 1H), 6.32 (d, $J=9.8$ Hz, 1H), 4.06 (s, 3H); $^{13}\text{C NMR}$ (126 MHz, DMSO- d_6): δ 160.0, 157.5, 147.8, 147.4, 147.4, 146.5, 143.1, 141.9, 131.2, 124.2, 121.0, 115.9, 114.2, 113.3, 112.7, 106.8, 61.6; **IR** (neat): 3257 (N-H), 3142 (C-H), 3065 (C=C), 2955 (C-H), 1720 (C=O), 1653 (C=O), 1590 (C=C), 1466 (N-H), 1423 (C=C), 1137 (C-O), 1170 (C-O) cm^{-1} ; **HRMS** (ESI $^+$): m/z calcd for $\text{C}_{17}\text{H}_{11}\text{NO}_6\text{Na}^+$ $[\text{M}+\text{Na}]^+$ 348.0484, found 348.0484.

***N*-(9-Methoxy-7-oxo-7H-furo[3,2-g]chromen-4-yl) thiophene-2-carboxamide (3h)**. The crude product was purified by silica gel column chromatography (eluent: 100%hexanes to EtOAc:hexanes=1:3) to provide the title compound. Green solid; 49% yield; **Mp**: 213–214 °C; **HPLC**: 98.42% purity; **TLC** (DCM:MeOH, 95:5 v/v): $R_f=0.50$; $^1\text{H NMR}$ (500 MHz, DMSO- d_6): δ 10.63 (br s, 1H), 8.09 (d, $J=3.3$ Hz, 1H), 8.08 (d, $J=2.2$ Hz, 1H), 8.01 (d, $J=9.8$ Hz, 1H), 7.88 (dd, $J=5.0, 0.9$ Hz, 1H), 7.24 (dd, $J=4.9, 3.8$ Hz, 1H), 6.90 (d, $J=2.2$ Hz, 1H), 6.42 (d, $J=9.9$ Hz, 1H), 4.16 (s, 3H); $^{13}\text{C NMR}$ (126 MHz, DMSO- d_6): δ 161.1, 159.8, 147.8, 147.3, 143.0, 141.8, 139.1, 132.6, 131.1, 130.4, 128.6, 124.0, 121.2, 114.3, 113.1, 106.7, 61.6; **IR** (neat): 3236 (N-H), 3123 (C-H), 2921 (C-H), 1725 (C=O), 1635 (C=O), 1590 (C=C), 1525 (N-H), 1414 (C=C), 1140 (C-O), 1098 (C-O), 718 (C-S) cm^{-1} ; **HRMS** (ESI $^+$): m/z calcd for $\text{C}_{17}\text{H}_{11}\text{NO}_5\text{SNa}^+$ $[\text{M}+\text{Na}]^+$ 364.0256, found 364.0261.

***N*-(9-Methoxy-7-oxo-7H-furo[3,2-g]chromen-4-yl)acetamide (3i)**. The title compound was synthesized following a slightly modified literature procedure³⁷ using **2** (24.0 mg, 0.10 mmol, 1.0 equiv.) in DCM (2.0 mL), a solution of acetic anhydride in DCM (1.00 mL, 1.0 mmol, 10.0 equiv.), pyridine (16 μL , 0.20 mmol, 2.0 equiv.) and DMAc (2.5 mg, 0.02 mmol, 0.2 equiv.), and K_2CO_3 (27.6 mg, 0.20 mmol, 2.0 equiv.). The crude product was purified by recrystallization with EtOH to provide the title compound. White solid; 42% yield; **Mp**: 251–252 °C; **HPLC**: 99.61% purity; **TLC** (DCM:MeOH, 95:5 v/v): $R_f=0.67$; $^1\text{H NMR}$ (500 MHz, DMSO- d_6): δ 10.06 (br s, 1H), 7.95 (d, $J=2.2$ Hz, 1H), 7.91 (d, $J=9.9$ Hz, 1H), 6.79 (d, $J=2.2$ Hz, 1H), 6.32 (d, $J=9.8$ Hz, 1H), 4.03 (s, 3H), 2.05 (s, 3H); $^{13}\text{C NMR}$ (126 MHz, DMSO- d_6): δ 169.5, 159.8, 147.3, 147.3, 142.9, 141.8, 130.6, 123.2, 122.0, 113.7, 112.2, 106.7, 61.4, 23.2; **IR** (neat): 3324 (N-H), 3114 (C-H), 2955 (C-H), 1709 (C=O), 1687 (C=O), 1593

(C=C), 1506 (N–H), 1163 (C–O), 1134 (C–O), 1058 (C–O) cm^{-1} ; **HRMS** (ESI⁺): m/z calcd for $\text{C}_{14}\text{H}_{11}\text{NO}_5\text{Na}^+$ [M+Na]⁺ 296.0535, found 296.0533.

N-(9-Methoxy-7-oxo-7H-furo[3,2-g]chromen-4-yl)propionamide (3j). The crude product was washed with hexanes to give the title compound. Gray solid; 64% yield; **Mp**: 233–234 °C; **HPLC**: 98.25% purity; **TLC** (DCM:MeOH, 95:5 v/v): $R_f=0.75$; **¹H NMR** (500 MHz, DMSO-*d*₆): δ 10.06 (br s, 1H), 8.03 (s, 1H), 7.96 (d, $J=9.8$ Hz, 1H), 6.83 (s, 1H), 6.40 (d, $J=9.8$ Hz, 1H), 4.10 (s, 3H), 2.42 (q, $J=7.4$ Hz, 2H), 1.12 (t, $J=7.4$ Hz, 3H); **¹³C NMR** (126 MHz, DMSO-*d*₆): δ 173.2, 159.8, 147.3, 147.2, 142.9, 141.7, 130.5, 123.1, 122.0, 113.7, 112.2, 106.6, 61.4, 28.9, 10.0; **IR** (neat): 3243 (N–H), 3118 (C–H), 2980 (C–H), 1719 (C=O), 1655 (C=O), 1591 (C=C), 1515 (N–H), 1425 (C=C), 1162 (C–O), 1135 (C–O) cm^{-1} ; **HRMS** (ESI⁺): m/z calcd for $\text{C}_{15}\text{H}_{13}\text{NO}_5\text{Na}^+$ [M+Na]⁺ 310.0691, found 310.0683.

N-(9-Methoxy-7-oxo-7H-furo[3,2-g]chromen-4-yl)isobutyramide (3k). The crude product was purified by silica gel column chromatography (eluent: EtOAc:hexanes = 1:3–1:1) to provide the title compound. White solid; 25% yield; **Mp**: 234–235 °C; **HPLC**: 99.19% purity; **TLC** (EtOAc:hexanes, 4:1): $R_f=0.53$; **¹H NMR** (500 MHz, CDCl₃): δ 7.70 (d, $J=9.8$ Hz, 1H), 7.62 (d, $J=2.2$ Hz, 1H), 7.50 (br s, 1H), 6.64 (d, $J=2.2$ Hz, 1H), 6.31 (d, $J=9.7$ Hz, 1H), 4.25 (s, 3H), 2.79–2.67 (m, 1H), 1.35 (d, $J=6.9$ Hz, 6H); **¹³C NMR** (126 MHz, CDCl₃): δ 176.4, 159.9, 147.3, 146.3, 142.9, 139.5, 131.8, 123.5, 118.8, 114.5, 112.8, 104.9, 61.3, 35.8, 19.7; **IR** (neat): 3248 (N–H), 3167 (C–H), 3129 (C=C), 2971 (C–H), 1732 (C=O), 1650 (C=O), 1588 (C=C), 1518 (N–H), 1161 (C–O), 1142 (C–O), 1128 (C–O) cm^{-1} ; **HRMS** (ESI⁺): m/z calcd for $\text{C}_{16}\text{H}_{15}\text{NO}_5\text{Na}^+$ [M+Na]⁺ 324.0848, found 324.0843.

N-(9-Methoxy-7-oxo-7H-furo[3,2-g]chromen-4-yl)pivalamide (3l). The crude product was purified by recrystallization with EtOH to provide the title compound. Yellow solid; 32% yield; **Mp**: 210–212 °C; **HPLC**: 97.01% purity; **TLC** (DCM:MeOH, 95:5 v/v): $R_f=0.40$; **¹H NMR** (500 MHz, DMSO-*d*₆): δ 9.65 (br s, 1H), 8.05 (s, 1H), 7.83 (d, $J=9.3$ Hz, 1H), 6.74 (s, 1H), 6.42 (d, $J=9.3$ Hz, 1H), 4.12 (s, 3H), 1.28 (s, 9H); **¹³C NMR** (126 MHz, DMSO-*d*₆): δ 178.0, 159.9, 147.6, 147.3, 142.9, 141.6, 130.8, 124.1, 122.4, 114.1, 113.2, 106.5, 61.5, 31.1, 27.7; **IR** (neat): 3215 (N–H), 3134 (C–H), 2984 (C–H), 1730 (C=O), 1640 (C=O), 1590 (C=C), 1505 (N–H), 1475 (C=C), 1376 (C–C), 1154 (C–O), 1133 (C–O) cm^{-1} ; **HRMS** (ESI⁺): m/z calcd for $\text{C}_{17}\text{H}_{17}\text{NO}_5\text{Na}^+$ [M+Na]⁺ 338.1004, found 338.1004.

N-Hexanoyl-*N*-(9-methoxy-7-oxo-7H-furo[3,2-g]chromen-4-yl)hexanamide (3m). The crude product was purified by silica gel column chromatography (eluent: EtOAc:hexanes = 1:9–1:2) to provide the title compound. White solid; 21% yield; **Mp**: 170–171 °C; **HPLC**: 97.31% purity; **TLC** (DCM:MeOH, 95:5 v/v): $R_f=0.67$; **¹H NMR** (500 MHz, CDCl₃): δ 7.71 (d, $J=2.3$ Hz, 1H), 7.54 (d, $J=9.8$ Hz, 1H), 6.61 (d, $J=2.3$ Hz, 1H), 6.44 (d, $J=9.9$ Hz, 1H), 4.35 (s, 3H), 2.57–2.50 (m, 4H), 1.67–1.57 (m, 4H), 1.31–1.16 (m, 8H), 0.84 (t, $J=7.0$ Hz, 6H); **¹³C NMR** (126 MHz, CDCl₃): δ 175.7, 159.3, 147.7, 147.0, 143.0, 137.9, 133.3, 125.5, 120.4, 116.6, 114.7, 103.8, 61.3, 38.0, 31.1, 24.2, 22.3, 13.7; **IR** (neat): 3441 (N–H), 3126 (C–H), 2953 (C–H), 2926 (C–H), 2858 (C–H), 1726 (C=O), 1685 (C=O), 1589 (C=C), 1480 (N–H), 1163 (C–O), 1135 (C–O) cm^{-1} ; **HRMS** (ESI⁺): m/z calcd for $\text{C}_{24}\text{H}_{31}\text{NO}_5\text{Na}^+$ [M+Na]⁺ 450.1893, found 450.1885.

(3*r*,5*r*,7*r*)-*N*-(9-Methoxy-7-oxo-7H-furo[3,2-g]chromen-4-yl)adamantane-1-carboxamide (3n). The crude product was purified by silica gel column chromatography (eluent: 100%hexanes to EtOAc:hexanes = 1:4) to provide the title compound. Off-white solid; 15% yield; **Mp**: 240–242 °C; **HPLC**: 97.53% purity; **TLC** (EtOAc:hexanes, 2:1): $R_f=0.48$; **¹H NMR** (500 MHz, CDCl₃): δ 7.62 (br s, 1H), 7.59 (d, $J=9.8$ Hz, 1H), 7.58 (d, $J=2.2$ Hz, 1H), 6.55 (d, $J=2.2$ Hz, 1H), 6.23 (d, $J=9.8$ Hz, 1H), 4.22 (s, 3H), 2.13 (s, 3H), 2.04 (d, $J=2.5$ Hz, 6H), 1.79 (q, $J=12.5$ Hz, 6H); **¹³C NMR** (126 MHz, CDCl₃): δ 177.6, 160.1, 147.4, 146.4, 143.0, 139.8, 131.7, 123.8, 119.5, 114.4, 113.0, 105.2, 61.5, 41.6, 39.5, 36.5, 28.2; **IR** (neat): 2953 (C–H), 1729 (C=O), 1640 (C=C), 1590 (C=C), 1133 (C–O) cm^{-1} ; **HRMS** (ESI⁺): m/z calcd for $\text{C}_{23}\text{H}_{23}\text{NO}_5\text{Na}^+$ [M+Na]⁺ 416.1468, found 416.1462; Data are consistent with literature values¹⁵.

4-(Benzylamino)-9-methoxy-7H-furo[3,2-g]chromen-7-one (4a). The title compound was synthesized following a slightly modified literature procedure¹⁵ using **2** (72.0 mg, 0.30 mmol, 1.0 equiv.) in anhydrous acetone (1.5 mL) benzyl bromide (43 μL , 0.36 mmol, 1.2 equiv.) and K₂CO₃ (63.0 mg, 0.45 mmol, 1.5 equiv.) at 55 °C overnight. The crude product was purified by silica gel column chromatography (eluent: 100%hexanes to EtOAc:hexanes = 2:3) to provide the title compound. Yellow solid; 21% yield; **Mp**: 168–169 °C; **HPLC**: 97.00% purity; **TLC** (EtOAc:hexanes, 1:1): $R_f=0.50$; **¹H NMR** (400 MHz, CDCl₃): δ 7.84 (d, $J=9.9$ Hz, 1H), 7.53 (d, $J=2.3$ Hz, 1H), 7.37–7.34 (m, 5H), 6.82 (d, $J=2.3$ Hz, 1H), 6.18 (d, $J=9.9$ Hz, 1H), 4.65 (s, 2H), 4.11 (s, 3H); **¹³C NMR** (101 MHz, CDCl₃): δ 160.6, 150.3, 144.7, 144.4, 138.8, 134.4, 129.0, 127.9, 127.5, 126.5, 114.3, 112.9, 111.2, 105.9, 104.6, 61.7, 52.5; **IR** (neat): 3421 (N–H), 3121 (C–H), 2932 (C–H), 1703 (C=O), 1585 (C=C), 1152 (C–O) cm^{-1} ; **HRMS** (ESI⁺): m/z calcd for $\text{C}_{19}\text{H}_{15}\text{NO}_4\text{H}^+$ [M+H]⁺ 322.1080, found 322.1078; Data are consistent with literature values¹⁵.

4-((4-Bromobenzyl)amino)-9-methoxy-7H-furo[3,2-g]chromen-7-one (4b). The title compound was synthesized with the same protocol as **4a** using 4-bromobenzyl bromide (48 μL , 0.36 mmol, 1.2 equiv.)¹⁵. The crude product was purified by silica gel column chromatography (eluent: EtOAc:hexanes = 1:9–2:1) to provide the title compound. Yellow solid; 39% yield; **Mp**: 150–151 °C; **HPLC**: 97.78% purity; **TLC** (EtOAc:hexanes, 1:1): $R_f=0.60$; **¹H NMR** (500 MHz, CDCl₃): δ 7.85 (d, $J=9.9$ Hz, 1H), 7.53 (d, $J=2.3$ Hz, 1H), 7.48 (d, $J=8.3$ Hz,

2H), 7.23 (d, $J=8.2$ Hz, 2H), 6.75 (d, $J=2.3$ Hz, 1H), 6.18 (d, $J=9.8$ Hz, 1H), 4.60 (s, 2H), 4.11 (s, 3H); $^{13}\text{C NMR}$ (126 MHz, CDCl_3): δ 160.7, 150.3, 144.8, 144.6, 138.9, 138.0, 134.2, 132.1, 129.2, 126.6, 121.8, 114.4, 111.4, 105.9, 104.8, 61.8, 51.7; **IR**: (neat): 3411 (N–H), 1691 (C=O), 1604 (C=C), 1530 (C=C), 716 (C–Br) cm^{-1} ; **HRMS** (ESI⁺): m/z calcd for $\text{C}_{19}\text{H}_{14}\text{BrNO}_4\text{H}^+$ [M+H]⁺ 400.0179, found 400.0169.

***N*-(9-Methoxy-7-oxo-7H-furo[3,2-g]chromen-4-yl)benzenesulfonamide (5).** The title compound was synthesized following a slightly modified literature procedure¹⁸ using **2** (47.0 mg, 0.20 mmol) in pyridine (400 μL); benzenesulfonyl chloride (30 μL , 0.22 mmol) and DMAP (2.5 mg, 0.02 mmol). The crude product was purified by silica gel column chromatography (eluent: EtOAc:hexanes = 1:4–3:1) to provide the title compound. Dark-green solid; 82% yield; **Mp**: 208–209 °C; **HPLC**: 98.02% purity; **TLC** (EtOAc:hexanes, 4:1): $R_f=0.53$; $^1\text{H NMR}$ (300 MHz, acetone- d_6): δ 9.07 (br s, 1H), 8.05 (d, $J=9.9$ Hz, 1H), 7.70 (d, $J=2.3$ Hz, 1H), 7.65–7.61 (m, 2H), 7.45 (t, $J=7.7$ Hz, 3H), 6.35 (d, $J=2.3$ Hz, 1H), 6.26 (d, $J=9.9$ Hz, 1H), 4.18 (s, 3H); $^{13}\text{C NMR}$ (75 MHz, acetone- d_6): δ 160.2, 148.3, 148.0, 144.6, 142.0, 140.4, 134.3, 133.4, 130.4, 128.4, 126.6, 120.1, 116.5, 115.1, 106.3, 61.9; **IR** (neat): 3201 (N–H), 3160 (C–H), 2951 (C–H), 1697 (C=O), 1615 (C=C), 1588 (C=C), 1474 (C=C), 1338 (S=O), 1164 (C–O), 1130 (C–O), 1053 (C–O), 724 (C–S) cm^{-1} ; **HRMS** (ESI⁺): m/z calcd for $\text{C}_{18}\text{H}_{13}\text{NO}_6\text{SNa}^+$ [M+Na]⁺ 394.0362, found 394.0365.

***1*-(5,9-Dimethoxy-7-oxo-6,7-dihydro-5H-furo[3,2-g]chromen-4-yl)-3-phenylthiourea (6).** The title compound was synthesized following a slightly modified literature procedure¹⁹ using **2** (47.0 mg, 0.20 mmol, 1.0 equiv.) in MeOH (1.0 mL), phenylisothiocyanate (90 μL , 2.22 mmol, 3.1 equiv.) under Ar atmosphere at 65 °C overnight. The crude product was purified by silica gel column chromatography (eluent: EtOAc:hexanes = 1:9–1:1) to provide the title compound. Dark-green solid; 49% yield; **Mp**: 191–192 °C; **HPLC**: 98.42% purity; **TLC** (EtOAc:hexanes, 2:3): $R_f=0.74$; $^1\text{H NMR}$ (400 MHz, CDCl_3): δ 8.82 (br s, 1H), 7.52 (d, $J=2.0$ Hz, 1H), 7.49–7.43 (m, 4H), 7.39 (t, $J=6.5$ Hz, 1H), 6.89 (d, $J=1.9$ Hz, 1H), 6.23 (br s, 1H), 5.50 (t, $J=5.0$ Hz, 1H), 4.15 (s, 4H), 3.55 (s, 4H), 3.00–2.74 (m, 2H); $^{13}\text{C NMR}$ (101 MHz, CDCl_3): δ 176.4, 170.2, 146.0, 144.0, 143.6, 140.4, 129.2, 128.6, 128.4, 128.1, 122.0, 108.6, 103.2, 103.0, 60.9, 57.2, 51.9, 38.4; **IR**: (neat): 3274 (N–H), 2940 (C–H), 1744 (C=O), 1721 (C=O), 1644 (C=C), 1477 (C–H), 1342 (S=O), 1068 (S=O), 1045 (S=O) cm^{-1} ; **HRMS** (ESI⁺): m/z calcd for $\text{C}_{20}\text{H}_{18}\text{N}_2\text{O}_5\text{SH}^+$ [M+H]⁺ 399.1015, found 399.1011.

Anti-cancer activity. *Cell lines.* MDA-MB-231 (triple-negative breast cancer) was obtained from M.D. Anderson Cancer Center, Houston, TX, USA). T47-D (hormone-dependent breast carcinoma), SK-BR-3 (human HER2+ breast cancer), and MRC-5 (normal embryonic lung fibroblast) were obtained from the American Type Culture Collection (ATCC, Manassas, VA, USA).

Cytotoxicity evaluation. The cytotoxic effect of tested compounds was evaluated in two breast cancer cell lines, MDA-MB-231 and T47-D. Number of survival cells after exposure to tested compounds for 48 h was determined by MTT assay, as previously described³⁸. The cancer selectivity of the tested compounds was demonstrated by comparing with cytotoxicity of a normal cell line, MRC-5. Three standard anti-cancer drugs, doxorubicin, tamoxifen citrate, and lapatinib, were used as positive controls in this assay.

Cancer chemopreventive activities. *Inhibition of aromatase (AIA).* Inhibition of the aromatase was performed using the method designed by Stresser et al.³⁹. The reference compound, letrozole, inhibited CYP19 with an IC_{50} value of 2.6 ± 0.1 nM.

For other cancer chemoprevention assays please see Supplementary.

Phototoxicity. SK-BR-3 and MDA-MB-231 cells were seeded into 96-well cell culture plates at 5×10^3 cells/well and incubated for 24 h at 37 °C under 5% CO_2 . After that, the cells were treated with 50 μM of psoralen derivatives in DMEM with 10% FBS and the cells were continued incubation for another 4 h. After incubation, the cells were washed with PBS (3 times) and then irradiated by a 365 nm lamp with the light intensity of 2.0 J cm^{-2} for 12.5 min before re-incubation for another 72 h. After incubation, the cell was treated with methylthiazolyldiphenyl-tetrazolium bromide (MTT reagent 200 μL , 0.5 mg mL^{-1} , Sigma-Aldrich) for 2 h. After reagent removal, DMSO was added to dissolve the formazan product and the cell viabilities were determined through UV–Vis absorption of the resulting formazan at wavelength 560 nm using a microplate reader (BMG Labtech/SPECTROstar Nano). The cell morphology images were captured by using a light microscope (Microscope Nikon, inverted digital) at 20X magnification prior to treating with MTT reagent.

Molecular docking studies. The protein HER2 co-crystallized with a small molecule inhibitor (PDB ID: 3PP0) was retrieved from the protein data bank (<https://www.rcsb.org/PDB>). Both protein and ligands were prepared using AutoDock Tools 1.5.7⁴⁰. The ligands and solvent molecules were removed, and polar hydrogen atoms were added. Tautomeric forms of histidine residues were set in accordance with the PQR computed with AMBER forcefield at pH 7.0 using APBS-PDB2PQR software suite (<https://server.poissonboltzmann.org/>)⁴¹. Two docking grid boxes were set as: box 1, center at (10,29,27) of size $x=28 \text{ \AA}$, $y=40 \text{ \AA}$, $z=20 \text{ \AA}$, and box 2¹¹, center at (9,24.5,42) of size $x=28 \text{ \AA}$, $y=48 \text{ \AA}$, $z=44 \text{ \AA}$. Both of the grid boxes gave similar results with no significant difference in most cases (see Supplementary Table S2). The exhaustiveness of conformational search is set to 16.

Molecular docking was performed using AutoDock Vina 1.1.2⁴⁰. The models were validated by redocking the co-crystallized ligand back into the binding site. The root mean-squared deviation (RMSD) between the

heavy atoms is calculated using obrms as implemented in openbabel^{42,43}. The top scoring predicted pose of the co-crystallized ligand has an RMSD of 0.60 Å (box 1) and 0.62 Å (box 2) compared with the X-ray pose. Docked poses were analyzed and figures were prepared using Obabel 3.1.1, Maestro 13.0, and PyMol 1.8^{44,45}.

The physicochemical properties. Drug-likeness properties and Lipinski's rule of five were obtained by using SwissADME website services^{46,47}.

Conclusions

Twenty psoralen derivatives with C-5 substitution were successfully synthesized, of which sixteen compounds were novel. Although the dark IC₅₀ towards breast cancer cells of these derivatives were relatively high, possibly due to the unusually low sensitivity of the cancer cell lines, some important structural features at C-5 can be deduced. In addition, these derivatives showed strong selectivity towards hormone-dependent T47-D compared to the hormone-independent MDA-MB-231, and low toxicity towards normal cells. Moreover, significant cancer chemopreventive activity through aromatase inhibition was also observed in some compounds. The presence of UVA irradiation led to a dramatic increase in the cytotoxicity, and the aliphatic and heteroaromatic amides were the most active with the IC₅₀ of up to 2.71 μM for **3g**. The extreme selectivity of the phototoxicity towards the HER2+ SK-BR-3 over the HER2- MDA-MB-231 suggested the HER2 as the possible target, which was further confirmed by the molecular docking study. Additionally, the cell morphology suggested that the significant inhibition of SK-BR-3 cells under UVA irradiation appeared to be related to induction of cell apoptosis. Finally, the physicochemical properties for most of the synthesized compounds are in the acceptable range for drug-likeness. The knowledge obtained from this work is crucial for the further development of anti-breast cancer agents based on the psoralen scaffold in the future.

Data availability

The datasets generated and/or analyzed during the current study are available in the supplementary file. The top scoring molecular docking poses of **8-MOP**, **3g**, and **3j** overlaid on HER2 protein structure (PDB ID: 3PP0, retrieved from the protein data bank, <https://www.rcsb.org/structure/3pp0>) are available in the open access repository, https://github.com/ruchuta/Molecular_Docking.

Received: 24 May 2022; Accepted: 28 July 2022

Published online: 05 August 2022

References

- Sung, H. *et al.* Global cancer statistics 2020: GLOBOCAN estimates of incidence and mortality worldwide for 36 cancers in 185 countries. *CA Cancer J. Clin.* **71**, 209–249. <https://doi.org/10.3322/caac.21660> (2021).
- Moo, T.-A., Sanford, R., Dang, C. & Morrow, M. Overview of breast cancer therapy. *PET Clin.* **13**, 339–354. <https://doi.org/10.1016/j.cpet.2018.02.006> (2018).
- Hale, M. J., Howell, A., Dowsett, M., Cuzick, J. & Sestak, I. Tamoxifen related side effects and their impact on breast cancer incidence: a retrospective analysis of the randomised IBIS-I trial. *Breast* **54**, 216–221. <https://doi.org/10.1016/j.breast.2020.10.015> (2020).
- Loprinzi, P. D. & Cardinal, B. J. Effects of physical activity on common side effects of breast cancer treatment. *Breast Cancer* **19**, 4–10. <https://doi.org/10.1007/s12282-011-0292-3> (2012).
- Herynk, M. H. & Fuqua, S. A. Estrogen receptors in resistance to hormone therapy. *Adv. Exp. Med. Biol.* **608**, 130–143 (2007).
- Panno, M. L. & Giordano, F. Effects of psoralens as anti-tumoral agents in breast cancer cells. *World J. Clin. Oncol.* **5**, 348–358. <https://doi.org/10.5306/wjco.v5.i3.348> (2014).
- Fitzpatrick, T. B., Tannenbaum, C., Pathak, M. A. & Parrish, J. A. Photochemotherapy of psoriasis with oral methoxsalen and longwave ultraviolet light. *N. Engl. J. Med.* **291**, 1207–1211. <https://doi.org/10.1056/NEJM197412052912301> (1974).
- Zarebska, Z. *et al.* Detection of DNA-psoralen photoadducts in situ. *Photochem. Photobiol.* **39**, 307–312. <https://doi.org/10.1111/j.1751-1097.1984.tb08182.x> (1984).
- Richard, E. G. The science and (lost) art of psoralen plus UVA phototherapy. *Dermatol. Clin.* **38**, 11–23. <https://doi.org/10.1016/j.det.2019.08.002> (2020).
- Panno, M. L. *et al.* Evidence that bergapten, independently of its photoactivation, enhances p53 gene expression and induces apoptosis in human breast cancer cells. *Curr. Cancer Drug Targets* **9**, 469–481. <https://doi.org/10.2174/156800909788486786> (2009).
- Xia, W. *et al.* Photo-activated psoralen binds the ErbB2 catalytic kinase domain, blocking ErbB2 signaling and triggering tumor cell apoptosis. *PLoS One* **9**, e88983. <https://doi.org/10.1371/journal.pone.0088983> (2014).
- Slamon, D. J. *et al.* Human breast cancer: correlation of relapse and survival with amplification of the HER-2/neu oncogene. *Science* **235**, 177–182. <https://doi.org/10.1126/science.3798106> (1987).
- Wu, S. B. *et al.* Antiproliferative and apoptotic activities of linear furoucoumarins from notopterygium incisum on cancer cell lines. *Planta Med.* **76**, 82–85. <https://doi.org/10.1055/s-0029-1185971> (2010).
- Hafez, O. M. *et al.* Synthesis and antitumor activity of some new xanthotoxin derivatives. *Eur. J. Med. Chem.* **44**, 2967–2974. <https://doi.org/10.1016/j.ejmech.2009.01.006> (2009).
- Chauthe, S. K., Mahajan, S., Rachamalla, M., Tikoo, K. & Singh, I. P. synthesis and evaluation of linear furanocoumarins as potential anti-breast and anti-prostate cancer agents. *Med. Chem. Res.* **24**, 2476–2484. <https://doi.org/10.1007/s00044-014-1312-6> (2015).
- Katritzky, A. R. & Taylor, R. Chapter 3 nitration. *Adv. Heterocycl. Chem.* **47**, 39–58 (1990).
- Fave, C. *et al.* Tunable electrochemical switches based on ultrathin organic films. *J. Am. Chem. Soc.* **129**, 1890–1891. <https://doi.org/10.1021/ja068143u> (2007).
- Murase, H., Senda, K., Senoo, M., Hata, T. & Urabe, H. Rhodium-catalyzed intramolecular hydroarylation of 1-halo-1-alkynes: regioselective synthesis of semihydrogenated aromatic heterocycles. *Eur. J. Med. Chem.* **20**, 317–322. <https://doi.org/10.1002/chem.201303008> (2014).
- Alawode, O. E., Robinson, C. & Rayat, S. Clean photodecomposition of 1-methyl-4-phenyl-1H-tetrazole-5(4H)-thiones to carbodiimides proceeds via a biradical. *J. Org. Chem.* **76**, 216–222. <https://doi.org/10.1021/jo1019859> (2011).
- Dai, X., Cheng, H., Bai, Z. & Li, J. Breast cancer cell line classification and its relevance with breast tumor subtyping. *J. Cancer* **8**, 3131–3141. <https://doi.org/10.7150/jca.18457> (2017).

21. Khan, S. I., Zhao, J., Khan, I. A., Walker, L. A. & Dasmahapatra, A. K. Potential utility of natural products as regulators of breast cancer-associated aromatase promoters. *Reprod. Biol. Endocrinol.* **9**, 1–10. <https://doi.org/10.1186/1477-7827-9-91> (2011).
22. Smith, I. E. & Dowsett, M. Aromatase inhibitors in breast cancer. *N. Engl. J. Med.* **348**, 2431–2442. <https://doi.org/10.1056/NEJMr023246> (2003).
23. Diawara, M. M. *et al.* A novel group of ovarian toxicants: the psoralens. *J. Biochem. Mol. Toxicol.* **13**, 195–203. [https://doi.org/10.1002/\(sici\)1099-0461\(1999\)13:3<4%3c195::aid-jbt10%3e3.0.co;2-p](https://doi.org/10.1002/(sici)1099-0461(1999)13:3<4%3c195::aid-jbt10%3e3.0.co;2-p) (1999).
24. McDermott, D. S., Hoyer, P. B. & Diawara, M. M. 8-Methoxypsoralen suppresses production of ovarian aromatase proteins. *Tox. Rev.* **24**, 235–245. <https://doi.org/10.1081/txr-200057861> (2005).
25. Panno, M. L. *et al.* Bergapten induces ER depletion in breast cancer cells through SMAD4-mediated ubiquitination. *Breast Cancer Res. Treat.* **136**, 443–455. <https://doi.org/10.1007/s10549-012-2282-3> (2012).
26. Acharya, R., Chacko, S., Bose, P., Lapenna, A. & Pattanayak, S. P. Structure based multitargeted molecular docking analysis of selected furanocoumarins against breast cancer. *Sci. Rep.* **9**, 1–13. <https://doi.org/10.1038/s41598-019-52162-0> (2019).
27. Dai, C.-L. *et al.* Lapatinib (Tykerb, GW572016) reverses multidrug resistance in cancer cells by inhibiting the activity of ATP-binding cassette subfamily B member 1 and G member 2. *Cancer Res.* **68**, 7905–7914. <https://doi.org/10.1158/0008-5472.CAN-08-0499> (2008).
28. García-Lainez, G., Vayá, I., Marín, M. P., Miranda, M. A. & Andreu, I. In vitro assessment of the photo(geno)toxicity associated with lapatinib, a tyrosine kinase inhibitor. *Arch. Toxicol.* **95**, 169–178. <https://doi.org/10.1007/s00204-020-02880-6> (2021).
29. Spielmann, H. *et al.* EEC/COLIPA project on in vitro phototoxicity testing: first results obtained with a BALB/c 3T3 cell phototoxicity assay. *Toxicol. In Vitro.* **8**, 793–796. [https://doi.org/10.1016/0887-2333\(94\)90069-8](https://doi.org/10.1016/0887-2333(94)90069-8) (1994).
30. Oldham, M. *et al.* X-ray psoralen activated cancer therapy (X-PACT). *PLoS One* **11**, e0162078. <https://doi.org/10.1371/journal.pone.0162078> (2016).
31. Aertgeerts, K. *et al.* Structural analysis of the mechanism of inhibition and allosteric activation of the kinase domain of HER2 protein. *Int. J. Biol. Chem.* **286**, 18756–18765 (2011).
32. Veber, D. F. *et al.* Molecular properties that influence the oral bioavailability of drug candidates. *J. Med. Chem.* **45**, 2615–2623. <https://doi.org/10.1021/jm020017n> (2002).
33. Clark, D. E. What has polar surface area ever done for drug discovery?. *Future Med. Chem.* **3**, 469–484. <https://doi.org/10.4155/fmc.11.1> (2011).
34. Sun, H. A universal molecular descriptor system for prediction of Log P, LogS, LogBB, and absorption. *J. Chem. Inf. Comput. Sci.* **44**, 748–757. <https://doi.org/10.1021/ci030304f> (2004).
35. Chen, X. *et al.* Analysis of the physicochemical properties of acaricides based on Lipinski's rule of five. *Comput. Biol.* **27**, 1–10. <https://doi.org/10.1089/cmb.2019.0323> (2020).
36. Zhang, B.-L., Fan, C.-Q., Dong, L., Wang, F.-D. & Yue, J.-M. Structural modification of a specific antimicrobial lead against *Helicobacter pylori* discovered from traditional chinese medicine and a structure-activity relationship study. *Eur. J. Med. Chem.* **45**, 5258–5264. <https://doi.org/10.1016/j.ejmech.2010.08.045> (2010).
37. Neises, B. & Steglich, W. Simple method for the esterification of carboxylic acids. *Angew. Chem. Int. Ed.* **17**, 522–524. <https://doi.org/10.1002/anie.197805221> (1978).
38. Thongnest, S., Boonsombat, J., Prawat, H., Mahidol, C. & Ruchirawat, S. Ailanthusins A-G and Nor-Lupane triterpenoids from *Ailanthus triphysa*. *Phytochemistry* **134**, 98–105. <https://doi.org/10.1016/j.phytochem.2016.11.007> (2017).
39. Stresser, D. M. *et al.* A high-throughput screen to identify inhibitors of aromatase (CYP19). *Anal. Biochem.* **284**, 427–430. <https://doi.org/10.1006/abio.2000.4729> (2000).
40. Trott, O. & Olson, A. J. AutoDock Vina: improving the speed and accuracy of docking with a new scoring function, efficient optimization and multithreading. *J. Comput. Chem.* **31**, 455–461. <https://doi.org/10.1002/jcc.21334> (2010).
41. Jurrus, E. *et al.* Improvements to the APBS biomolecular solvation software suite. *Protein Sci.* **27**, 112–128. <https://doi.org/10.1002/pro.3280> (2018).
42. O'Boyle, N. M. *et al.* Open babel: An open chemical toolbox. *J. Cheminform.* **3**, 1–14. <http://www.jcheminf.com/content/3/1/33> (2011).
43. The Open Babel Package, version 2.3.1 <http://openbabel.org>.
44. Maestro 13.0, Schrödinger, LLC, New York, NY, 2021 <https://www.schrodinger.com/products/maestro>.
45. The PyMOL Molecular Graphics System, Version 1.8 Schrödinger, LLC. <https://pymol.org/2/>.
46. Pires, D. E., Blundell, T. & Ascher, D. pkCSM: Predicting small-molecule pharmacokinetic and toxicity properties using graph-based signatures. *J. Med. Chem.* **58**, 4066–4072. <https://doi.org/10.1021/acs.jmedchem.5b00104> (2015).
47. Daina, A., Michielin, O. & Zoete, V. SwissADME: A free web tool to evaluate pharmacokinetics, drug-likeness and medicinal chemistry friendliness of small molecules. *Sci. Rep.* **7**, 42717. <https://doi.org/10.1038/srep42717> (2017).

Acknowledgements

This research is funded by The Asahi Glass Foundation under CU-AGF Grant 2022; Office of the Permanent Secretary, Ministry of Higher Education, Science, Research and Innovation (OPS MHESI), Thailand Science Research and Innovation (TSRI) (Grant No. RGNS 64-008); the Suranaree University of Technology (SUT); the Thailand Science Research and Innovation (TSRI); Chulabhorn Research Institute (Grant No. 2536703/42320); and Center of Excellence on Environmental Health and Toxicology (EHT), OPS, Ministry of Higher Education, Science, Research and Innovation. We thank the following CRI staff members, Pakamas Intachote, Suchada Sengsai, and Busakorn Saimanee for carrying out the cytotoxic activity evaluation; and Somkid Sitthimonchai for bioassays on cancer chemopreventive activity. We also thank Asst. Prof. Dr. Warinthorn Chavasiri for the supervision. The Scholarship from the Graduate School, Chulalongkorn University to commemorate the 72nd anniversary of his Majesty King Bhumibol Aduladej is gratefully acknowledged.

Author contributions

Conceptualization, J.B., T.K.; data curation, J.B., T.K.; formal analysis, A.K., R.A., S.T., J.B., T.K.; funding acquisition, J.B., T.K.; investigation, C.A., S.W., R.A., S.T.; methodology, C.A., A.K., R.A., S.T., J.B., T.K.; project administration, J.B., T.K.; resources, S.R.; software, R.A.; supervision, S.R.; validation, A.K., R.A., S.T., J.B., S.R., T.K.; visualization, C.A., S.W., R.A., T.K.; writing-original draft preparation, C.A., J.B., T.K.; writing-review and editing, A.K., R.A., J.B., S.R., T.K.; All authors have read and agreed to the published version of the manuscript.

Competing interests

The authors declare no competing interests.

Additional information

Supplementary Information The online version contains supplementary material available at <https://doi.org/10.1038/s41598-022-17625-x>.

Correspondence and requests for materials should be addressed to J.B. or T.K.

Reprints and permissions information is available at www.nature.com/reprints.

Publisher's note Springer Nature remains neutral with regard to jurisdictional claims in published maps and institutional affiliations.



Open Access This article is licensed under a Creative Commons Attribution 4.0 International License, which permits use, sharing, adaptation, distribution and reproduction in any medium or format, as long as you give appropriate credit to the original author(s) and the source, provide a link to the Creative Commons licence, and indicate if changes were made. The images or other third party material in this article are included in the article's Creative Commons licence, unless indicated otherwise in a credit line to the material. If material is not included in the article's Creative Commons licence and your intended use is not permitted by statutory regulation or exceeds the permitted use, you will need to obtain permission directly from the copyright holder. To view a copy of this licence, visit <http://creativecommons.org/licenses/by/4.0/>.

© The Author(s) 2022